Developing a Novel Cell Surface RNA Detecting Method via RNA Metabolic Labeling

Maxwell David Brooks

Thesis submitted to the faculty of the Virginia Polytechnic Institute and State University

in partial fulfillment of the requirements for the degree of

Master of Science in Life Science in Biochemistry

Wei Sun, Chair

Pablo Sobrado

Andrew N. Lowell

May 1st, 2024

Blacksburg, VA

Keywords: Cell Surface RNA, Assay Development, RNA Biology, Molecular Biology,

Metabolic Labeling

Developing a Novel Cell Surface RNA Detecting Method via RNA Metabolic Labeling

Maxwell David Brooks

ABSTRACT

Cell surface RNA (csRNA) is a recent discovery in the field of RNA biology and has been implicated in playing important roles in many biological processes due to its extracellular properties. To understand the biogenesis, regulation, and function of csRNA, it is critical to develop methods to detect, isolate, and confidently characterize membrane-bound csRNA. Previously, csRNA has been profiled using methods based on cell membrane isolation that are expensive, laborious, and with unsatisfactory specificity and sensitivity. In this study, we use metabolic labeling and chemical cross-linking techniques to specifically label csRNA with biotin handles. We intended to use this technique for separating biotin-labeled csRNA from total RNA samples for characterization purposes. The primary materials that were used to label such csRNAs are 4-Thiouridine (4sU), an unnatural nucleotide analogue, and S-(2-aminoethyl)-ester-methanesulfonothioic-acid-biotin (MTSEA-biotin), a crosslinker designed specifically to label 4sU. By deploying these tools to cell lines such as HEK293T and HeLa, csRNA is detectable by Enhanced Chemiluminescent detection via Dot Blot. Furthermore, to separate biotin-labeled csRNA from total RNA, streptavidin-coated magnetic bead separation procedures could be used as a promising method for purifying csRNA from total RNA, for RNAseq characterization. This study highlights the processes of establishing the csRNA detection protocol and describes the current status and issues with developing the streptavidin-coated magnetic beads separation method.

Developing a Novel Cell Surface RNA Detecting Method via RNA Metabolic Labeling

Maxwell David Brooks

GENERAL AUDIENCE ABSTRACT

The ‘central dogma’ is a term that describes the process of DNA (a template-like molecule that holds all genetic coding within cells) transcribing into mRNA (a messenger molecule that transports this message to the ribosome) which is then translated into proteins (large, complex molecular machinery that is responsible for many biochemical functions within the body). However, RNA has been found to have a much wider range of functions than just being an intermediate messenger between DNA and proteins. Recently, short snippets of single nucleotide RNA strands have been discovered to be present on the outer cell membrane of certain mammalian cell types. The function of cell surface RNA (csRNA) is largely undiscovered, however, csRNA are likely involved in cell-cell interactions similar to outer membrane proteins, lipids, and carbohydrates. Currently, methods involved in detecting and characterizing csRNA are laborious, time extensive, and with unsatisfactory specificity and sensitivity. This study aims to develop novel methods to detect csRNA on different cell types in an undemanding and trustworthy manner to speed up research timelines while maintaining high confidence in results. Our design is to use metabolic labeling and click-chemistry to ‘label’ the csRNA. In this study, we describe early signs of detecting csRNA and how this was achieved. Additionally, the current status for separating and profiling csRNA sequences is discussed.

Acknowledgements:

I would like to acknowledge the entire Sun Lab for helping me throughout this process of starting the project. The lab itself is only a year and a half old, therefore many protocols and instruments had to be troubleshooted, let alone written up. The natural culture of wanting to help one another, and never saying no to a favor really helped build this research from the ground up. Thank you Pabina, Geoffery, and Matt for being a helping hand and allowing me to share ideas for discussion throughout the troubleshooting process. Thank you, Dr. Sun, for giving me the opportunity to help create a base system of lab duties, standard operating procedures, and an initial layer of research. Thank you to all the undergrads who seemed genuinely interested in the science. Due to the lack of the lab having previous grad students, undergraduates have worked hard to provide extra leg work for our research. I would also like to thank the Department of Biochemistry and the Graduate School of Virginia Tech who have recruited me and helped financially with the stipends we are given. Lastly, I would like to thank my family, specifically my father Mike and mother Sunshine who have supported me throughout this entire process and encouraged me to receive higher education.

Table of Contents

Chapter 1:

Introduction:

Ribonucleic acid (RNA) in previous history of research has been overshadowed by its complement, DNA. Recently, scientists have delved into the world of RNA biology and revealed the overlooked molecule as highly versatile with a far more expansive role than simply carrying genetic codes for protein translation in the form of mRNA (Mattick et al., 2023; D. Wang & Farhana, 2023). Certain unique RNA molecules have shown to adopt diverse structures and perform many different functions within the cell, including enzymatic reactions (D. Wang & Farhana, 2023). Exploring RNA in its various forms and functions may reveal important missing pieces to biomolecular mechanisms that have been shielded before.

As mentioned, mRNA serves as the blueprint for protein construction. However, other RNA structures have already been discovered to play critical roles in cellular processes. Some of the more commonly known types of RNA are transfer RNA (tRNA, acts as an adapter molecule carrying amino acids to the ribosome for protein assembly) (D. Wang & Farhana, 2023), Ribosomal RNA (rRNA provides structure and function of the ribosome core) (D. Wang & Farhana, 2023), microRNAs and small interfering RNAs (miRNAs/siRNAs regulate gene expression) (D. Wang & Farhana, 2023) and long non-coding RNAs (lncRNAs have a diverse set of functions such as gene expression, modifying chromatin, and protein localization)(Mattick et al., 2023). More information involving unique RNA structures as a major contributor to molecular cell mechanisms continues to arise, indicating the recently newfound importance of RNA biology outside of mRNA.

A recent and interesting discovery has challenged the original concepts of RNA localization and expression. Just within the past 5 years, researchers have identified the presence of RNA molecules on the outer membrane of specific mammalian cell types (Flynn et al., 2021; Huang et al., 2020; Lv et al., 2023; Ma et al., 2023; Zhang et al., 2024). These RNA molecules do not include incapsulated RNAs in extracellular vesicles or cell-free RNA, but specifically RNA that is anchored on the cell membrane and facing extracellularly, like many receptor proteins (Morozkin et al., 2004; Xie et al., 2019) Discovering nucleotide formations on the outer cell surface is rare and unexpected (Casciola-Rosen et al., n.d.). Many cell surface RNAs (csRNA) carry carbohydrate modifications, which are also named as glycoRNAs (Flynn et al., 2021). csRNA existence raises curiosity as to why evolution has come to develop a mechanism to anchor and present RNA molecules on the outsides of the cell membrane. Like many molecules found on the cell surface, csRNA was speculated to have functions involving cell-cell communication, immune response activity, or adhesion/cohesion properties that help guide intercellular communication as shown in Figure 1 (Flynn et al., 2021; Zhang et al., 2024). The latest research on csRNA particularly focuses on the role of glycosylated csRNAs in neutrophil recruitment and has shown that glycosylated csRNAs are necessary for the cellular localization of immune cells at sites of inflammation (Zhang et al., 2024). Due to the birth of this field being so recent, a more in-depth understanding is needed to uncover the molecular function of csRNA. Laying a new foundation of procedures for csRNA detection and profiling can pave the way for subsequent research focusing on csRNA cell-type specificity (Block et al., 2011).

Figure 1:

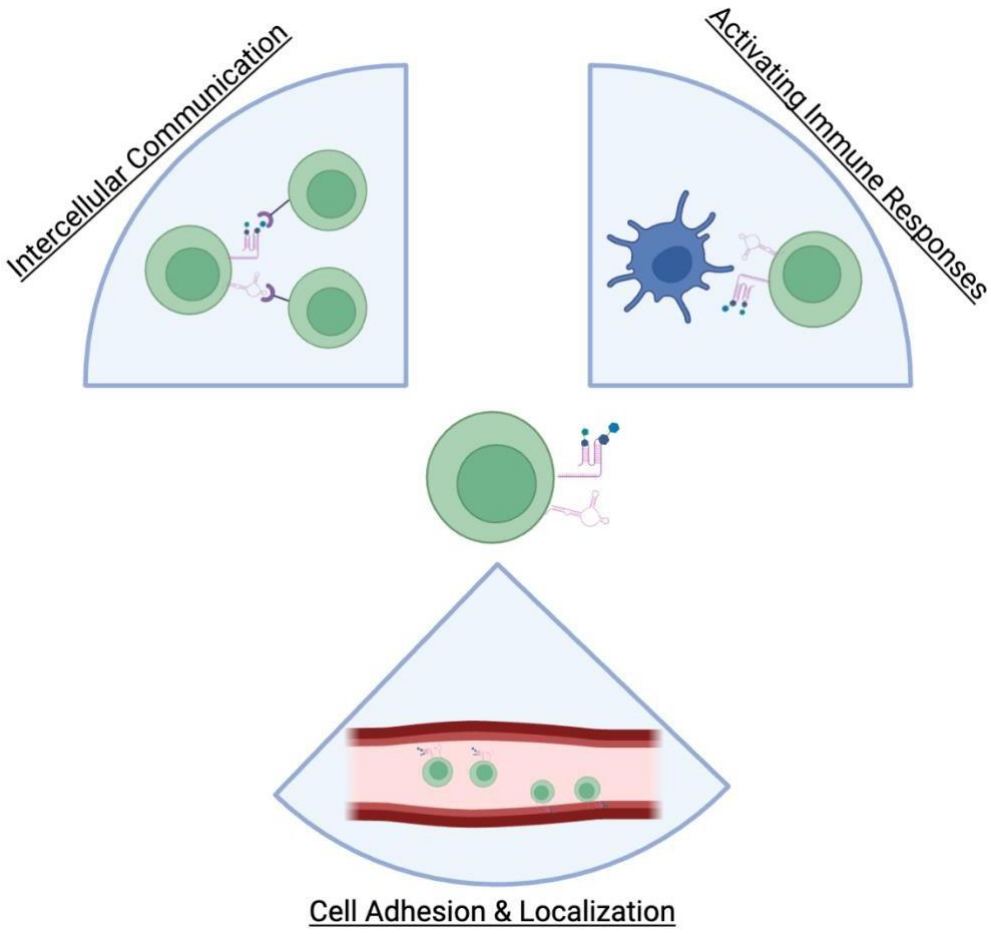

Fig. 1: Visual representation highlighting the hypothesis describing possible functions of csRNA, including intercellular signaling similar to protein or sugar ligand presenting cells, eliciting immune responses recognizable by innate or adaptive immune cells, and/or cell adhesion & localization of specific cell types.

Currently, csRNA are so far observed on CD14+ monocytes, dendritic cells, neutrophils, and immortal cancer cell lines (HEK293T, HELA, EL4) (Flynn et al., 2021; Huang et al., 2020; Lv et al., 2023; Ma et al., 2023; Zhang et al., 2024). There are many remaining questions revolving around csRNA such as: how are they transported to the cell surface? How are they anchored to the outer cell membrane? And how do they impact cell membrane function? Discovery of csRNA

could reveal undiscovered cell-cell interactions that are critical to immune function and disease. Moreover, using csRNA profiles to deliver drugs specific for some diseases could lead to novel therapy innovations (Manya et al., 2016; Praissman et al., 2016). If csRNA sequences are unique to cell types, then csRNA could be employed as a "molecular zip-code" for targeted drug delivery.

Recently, researchers have relied on antibodies, DNA probes, and sugar metabolic labeling to detect and visualize csRNA (Figure 2) (Flynn et al., 2021; Huang et al., 2020; Lv et al., 2023; Ma et al., 2023; Zhang et al., 2024). Isolating RNA from total cell lysate often involves harsh techniques that use detergents (Chomczynski & Sacchi, 2006a). This process would denature any proteins that are bound to RNA molecules, making antibodies obsolete for csRNA separation and profiling via RNA sequencing (RNAseq). Previous methods to separate and profile csRNA is a laborious process which may end in false positive results (Huang et al., 2020; Lv et al., 2023). To physically separate csRNA from total RNA for sequencing, methods rely on destroying the cell membrane and then reconstruct it (Figure 2) (Huang et al., 2020). First, researchers must homogenize the entire cell population which essentially means breaking down the cellular components into one mixture (Huang et al., 2020; Lv et al., 2023). This process may affect the natural interactions between cell membranes and RNA molecules, which could alter profiling results. Following homogenization, the membrane particles can be ligated back together in attempt to create lipid nanoparticles that still acquire bound csRNA (Huang et al., 2020). This process remains an unreliable and indirect method for the isolation and downstream sequencing of csRNA, because the labeling occurs *after* homogenization of the cells. Therefore, the insurance that transcripts sequenced are in fact outward facing membrane bound RNAs rather than inward

is at low confidence. Clear limitations exist in current methods for detecting and characterizing csRNA, providing urgent need for developing other detection and profiling methods.

Figure 2:

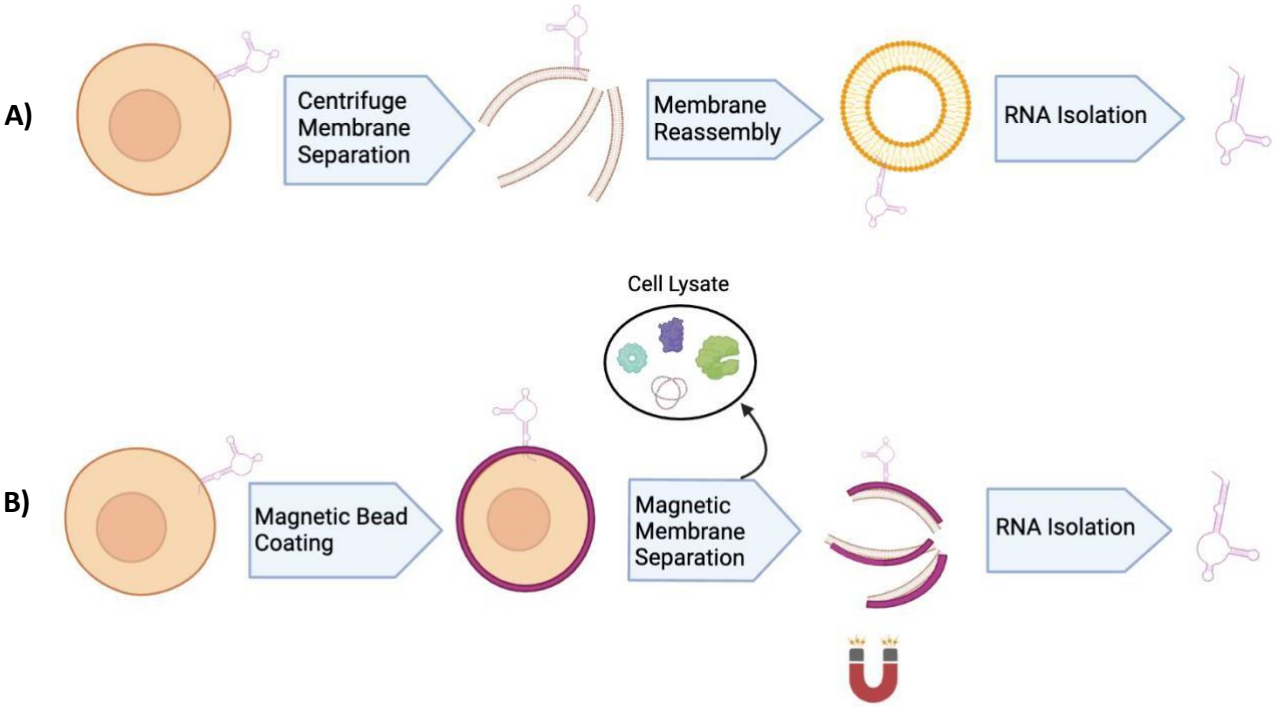

Fig. 2: Schematic showing the current processes for separating membrane bound RNA for profiling. ***A*** *- Membrane separation via centrifugation and reconstruction of the membrane into nanoparticles for extracellular RNA isolation.* ***B*** *- Magnetic coating of the cell membrane followed by magnetic separation of membrane from cell lysate for RNA isolation (cannot differentiate inner facing vs. outer facing membrane bound RNA.)*

Covalent crosslinking offers a compelling alternative compared to antibodies and homogenization/membrane nanoparticle reassembly for detecting and profiling purposes (Chomczynski & Sacchi, 2006b; Harris & Christian, 2009)By directly tagging csRNA with a biotin

containing crosslinker, researchers can bypass the difficult and potentially damaging method of homogenization and membrane particle recreation, because crosslinkers act like molecular bridges that can form covalent bonds between the csRNA and other molecules (Duffy et al., 2015; Garibaldi et al., 2017; Lamandé Editor, 2018). Often, this other molecule is biotin which can be used as a handle, detectable via of chemiluminescent assays, but could also be swapped with a fluorescent tag for imaging (Duffy et al., 2015; Garibaldi et al., 2017; Lamandé Editor, 2018). The covalent linkage between csRNA and a programmable tag molecule allows for not only visualization through fluorescent imaging techniques but also the potential for future isolation and sequencing (Duffy et al., 2015). Additionally, the resulting linkage between each molecule ensures a more reliable profile analysis due to its specificity, and the crosslinking occurs before homogenization of the cells which provides a more realistic snapshot of csRNA (Rabani et al., 2011). Thus, covalent crosslinking provides an all-in-one method that can provide visualization, detection, and separation of csRNA . This innovative approach has the potential to help accelerate the process of csRNA structure and function discovery (Rabani et al., 2011). To further understand cross-linking technology, basic understanding of metabolic labeling and click-chemistry is necessary.

To study RNA cellular dynamics, scientists have developed new ways to detect, track, and measure RNA abundance within living cells which can also be applied to csRNA research. Metabolic labeling, the technique used to label new transcripts of RNA, involves introducing modified nucleotides with special chemical groups into the cell culture media (Duffy et al., 2015; Garibaldi et al., 2017; Lamandé Editor, 2018). These modified nucleotide analogues are then incorporated by RNA polymerase into newly developed RNA molecules *in vivo*. 4-thiouridine

(4sU), one of the nucleotide analogues utilized in this study, has allowed researchers to distinguish newly transcribed RNA from pre-existing RNA (Garibaldi et al., 2017; Lamandé Editor, 2018). This nucleotide analogue is special due to the sulfhydryl group presented on the uridine base which allows for the addition of a crosslinker to bind to and label RNA transcripts (Figure 3). Metabolic labeling provides the molecular handle for click chemistry to occur for labeling purposes.

Click chemistry is a very powerful tool within molecular biology studies that offers a way to link molecules together for labeling purposes (Duffy et al., 2015; Garibaldi et al., 2017; Lamandé Editor, 2018). Click-chemistry crosslinkers are selectively designed molecules that can bind to metabolic labelers, such as 4sU (Figure 3). In all cases, a crosslinker contains a functional group specific towards a unique chemical group that readily reacts with each other, forming a covalent bond. These crosslinkers can be attached to biomolecules of interest, such as RNA, and used as a handle for detection and separation purposes. (Harris & Christian, 2009). When the functional groups of both a crosslinker and a metabolic labeler such as 4sU react, the crosslinker bridges the gap between the two molecules, giving the term “click-chemistry”. Combing metabolic labeling and click-chemistry principle gives reason to how RNA is studied and further supports the rationale behind applying this to csRNA research.

For research of csRNA specifically, MTSEA (methanethiosulfonate ethyl-maleimide) crosslinkers could potentially offer a very fast covalent reaction (Figure 3)(Duffy et al., 2015). This MTSEA crosslinking mechanism involves the methanethiosulfonate warhead group to react with free thiol (-SH) groups, such as the one found on 4sU, making it suitable for labeling RNA (Figure 3) (Duffy et al., 2015). The quick reaction time of MTSEA streamlines the labeling process,

minimizing disruptions to cellular functions (Duffy et al., 2015). Furthermore, MTSEA crosslinkers are impermeable to cell membranes (Duffy et al., 2015). Therefore, MTSEA primarily reacts with accessible thiol groups that are present on the cell surface. This selectivity is why MTSEA crosslinkers becomes so advantageous to labeling csRNAs. Since MTSEA cannot penetrate the cell membrane, it won't react with the intracellular RNAs labeled with 4sU. This greatly eliminates false positives during the detection and visualization of csRNA. Additionally, this provides selectivity when csRNA needs to be separated from total RNA for sequencing and profiling purposes (J. Wang et al., 2024; Z. Wang et al., 2009). The combination of selectivity and rapid reactivity makes MTSEA-biotin crosslinking befitting to label 4sU containing csRNA. In this research, two types of MTSEA crosslinkers were tested: MTSEA-biotin, and MTSEA-xx-biotin (Figure 3) (xx indicates a longer ethyl-maleimide for ensured impermeability).

Figure 3:

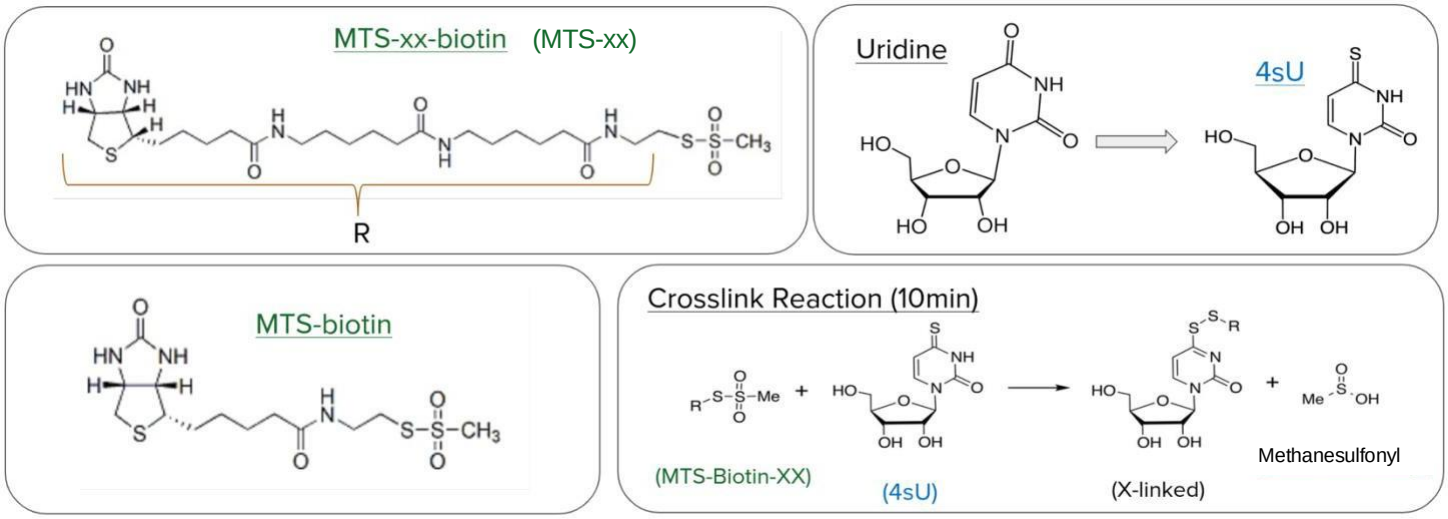

Fig. 3: ***A*** *- Chemical compounds proposed for labeling csRNA: MTS-xx-biotin (also referred to as MTS-xx), MTS-biotin, 4sU (4-thiouridine). Fast crosslinking reaction of MTSEA with sulfhydryl group of 4sU, resulting in loss of methanesulfonyl group.* ***B*** *- Representation of MTSEA-biotin compounds being impermeable and only reacting with csRNA containing 4sU and not intercellular transcripts.*

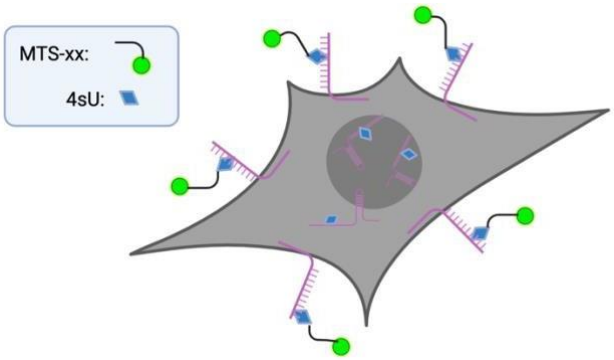

A critical gap of understanding csRNA structure and function is very intriguing. Current methods for detecting profiling these csRNAs remain separate processes and are prone to limitations (Huang et al., 2020; Lv et al., 2023). Therefore, this research aims to develop a method for the covalent crosslinking of metabolically labeled csRNA. This new approach involves incorporating the 4sU nucleotide analogue into newly synthesized csRNA molecules (Garibaldi et al., 2017; Lamandé Editor, 2018). Subsequently, a crosslinking agent would be introduced. The unique functional groups on MTSEA crosslinkers are designed to react specifically with the

sulfhydryl groups found within the 4sU analogues that are embedded into the csRNA transcripts (Duffy et al., 2015). This reaction would create a covalent bond between the csRNA and the crosslinking agent, effectively tagging the csRNA molecule that will stay intact throughout homogenization of cells and RNA phase isolation procedures. Our rationale provides extensive promise for speeding up csRNA research and would provide a more robust and complete approach for detecting and profiling csRNA molecules.

Literature Review:

i. Natural display of nuclear-encoded RNA on the cell surface and its impact on cell interaction (2020):

This is one of the first publications identifying RNA existing on the cell surface to pave the way for further research on extracellular presenting RNA. In this paper, they named cell surface RNA as maxRNA, which stands for membrane associated extracellular RNAs (Huang et al., 2020). The researchers were driven by the question of whether RNA could be displayed on the cell surface, and if so, what its functional implications might be. The investigation began by establishing the existence of maxRNA. Using Surface-seq and RNA-FISH techniques, they successfully identified and validated maxRNA molecules on the cell surface (Huang et al., 2020).

The first step of Surface-seq technique involves isolating the plasma membrane from the rest of the cellular components. Next, nanoparticle technology is used where the isolated plasma membrane is wrapped around polymeric cores, forming membrane-coated nanoparticles (MCNPs) (Huang et al., 2020). This step is said to preserve the original orientation of the membrane, ensuring that surface molecules remain facing outwards including the maxRNA. RNA molecules are then extracted from the MCNPs after they are formed (Huang et al., 2020). These extracted RNA molecules are then sequenced to identify the specific types of RNA present on the cell surface. RNA-FISH (RNA Fluorescence In Situ Hybridization) is a powerful technique that was also used within this study to visualize and localize specific RNA molecules within a cell (Huang et al., 2020). Ultimately, RNA-FISH provides a valuable tool for researchers to study RNA expression patterns, localization, and dynamics within cells and between different cell types.

These techniques revealed that maxRNA presentation was not uniform across all cell types. Monocytes and dendrites appeared to have preferential expression of maxRNA, potentially linking to unique, alternative roles in cell-cell interactions (Huang et al., 2020). The genes associated with maxRNA production also aligned with these functions, including those involved in cell adhesion and extracellular matrix remodeling (Huang et al., 2020).

A major challenge in studying maxRNA, shared between not only this research lab but all labs studying cell surface RNA, is its vulnerability to degradation by extracellular RNases. The researchers propose that steric hindrance by membrane proteins and lipids protects maxRNA fragments from further enzymatic breakdown, explaining why sequencing data revealed short RNA fragments rather than full-length transcripts (Huang et al., 2020).

This paper also explored the anchoring mechanisms for maxRNAs on the cell surface. Three plausible models were suggested, that being, formation of ribonucleoprotein complexes with transmembrane proteins, covalent linkage with surface glycans, and binding with membrane lipids (Huang et al., 2020). Functional roles of maxRNA have yet to be determined, but there are some hypotheses suggested by this research in what functions these RNAs have. maxRNAs within a ribonucleoprotein complex might help anchor associated proteins on the cell membrane, influencing their membrane-related functions (Huang et al., 2020). Additionally, some maxRNAs may modulate local membrane permeability (Huang et al., 2020). This aligns with claims from this article that synthetic RNAs can bind to the cell membrane, alter permeability to small molecules, and even form temporary channels for larger molecules.

However, the method used could exhibit false positives due to relying on homogenizing the entire cell population and reconstructing membrane nanoparticles (Huang et al., 2020).

Homogenization is a disruptive process which alters cellular structure and may potentially damage RNA molecules, especially those associated with the outer membrane. This can lead to degradation, causing a decrease or a complete loss of valuable csRNA. Furthermore, homogenization disrupts the natural organization of cellular components, potentially affecting the data produced and skewing understanding of csRNA structure and function. Following homogenization, the method attempts to reconstruct membrane particles, but is considered difficult to achieve purity for the method is known to be prone to contamination (Huang et al., 2020).

The entire process is not only inefficient but also time-consuming. This drawn-out approach limits sample processing and exhibits variability due to the extended handling time (Huang et al., 2020). The multiple limitations present in this current method highlights the need for alternative approaches for isolating csRNA.

Key Takeaway: csRNA discovery has pioneered a new area of research that may uncover misunderstood biochemical processes. The current method being used to profile csRNA requires homogenization of the cell culture and re-assembly of the membrane before RNA isolation and sequencing, making this laborious and messy protocol in need of amendment. (Huang et al., 2020)

ii. A Novel Cell Membrane-Associated RNA Extraction Method and Its Application in the Discovery of Breast Cancer Markers (2023):

The interesting concept that RNA has many more functionality than as a messenger for protein translation has attracted scientists to further study different types of RNA and their roles in molecular processes. Recent discoveries have further expanded our understanding of RNA's reach, including the discovery of RNA presenting on the cell surface. However, significant gaps remain in our knowledge of membrane bound RNAs. The researchers in this article create methods for extracting these mysterious RNA molecules (Lv et al., 2023).

The article explores a novel method for membrane associated RNA extraction that addresses previous method's limitations. The approach developed uses magnetic nanobeads to coat the cell membrane, therefore when the cell population is lysed, the beads block molecular interactions which increases the confidence in high-purity cell membranes (Lv et al., 2023). This works due to the positively charged cationic beads that interact electrostatically with the cell membrane, effectively capturing it after cell disruption (Lv et al., 2023).

However, there are some limitations to this study. The researchers primarily rely on enriching long non-coding RNAs as markers for cancer (Lv et al., 2023). While these findings are valuable, they lack a more comprehensive analysis of the cell surface RNA profiles. This may include other RNA species like microRNAs and small interfering RNAs that could provide a deeper understanding of their role in breast cancer, or even provide more possible therapeutic targets. Additionally, their method involves the separation of plasma membrane fragments from other cellular components (Lv et al., 2023). The RNA bound to these membrane fragments are then separated further for analysis. Therefore, their results include membrane bound RNA that face

both on the extracellular and interior side of the membrane. The distinction on which way the membrane bound RNA faces is an important aspect when applying this data towards therapeutic development.

Key Takeaway: csRNA can uniformly and uniquely be overexpressed on certain cell types, such as breast cancer tissue (Lv et al., 2023). The method used in this study profiles membrane bound RNA by deploying a magnetic bead coating to the membrane, allowing for isolation of the membrane and protection during homogenization. However, isolating RNA from the membrane results in profiling of membrane bound RNA that could be facing the cell's interior which fails to distinguish extracellular csRNA. (Lv et al., 2023).

iii. Small RNAs are modified with N-glycans and displayed on the surface of living cells (2021):

Carolyn R. Bertozzi, who has recently won the Nobel prize in chemistry in 2022 for her contribution for developing biorthogonal reactions, and Ryan A. Flynn dive into the exciting and relatively unexplored territory of glycan-RNA interactions (Flynn et al., 2021). This study by Flynn and Bertozzi discovered a new twist on regulatory RNA molecules within cells. These RNAs, typically lacking any coding function, were found to be conjugated with a N-glycan sugar chains (Flynn et al., 2021). Glycans, complex sugar molecules, play a critical role in various cellular functions. Relative function of these glycans is especially important on the cell surface. The sugars are known to help proteins and lipids fold correctly and are involved in molecule transportation mechanisms both intercellularly and intracellularly, such as secretion or

membrane incorporation (Flynn et al., 2021). Other processes like embryonic development, immune response to pathogens, and tumor-immune interactions all depend heavily on glycosylation (Flynn et al., 2021).

Another essential biopolymer, RNA, is a fundamental molecule necessary in all life forms. The building blocks of RNA consists of just four nucleotide bases; however, RNA can undergo extensive modifications after it's transcribed. These modifications, called post-transcriptional modifications, significantly increase the chemical diversity of RNA. Over 100 such modifications have been identified (Flynn et al., 2021). This complexity allows RNA to play various roles beyond its traditional function as a messenger molecule (mRNA) for further translation into proteins. RNA may also act as structural scaffolds, decoy molecules, enzymes, and a regulatory signaler within the cell (Flynn et al., 2021).

The authors previously developed methods to identify glycans associated with proteins using metabolic labeling and a special chemical reaction strategy, an example of biorthogonal chemistry that Bertozzi won the Nobel Prize for (Flynn et al., 2021). This method involves incorporating a specific tag (azide group) into naturally produced sugar molecules of the cell. This tag allows them to later attach a biotin molecule for easy detection and analysis. Interestingly, when they used this method with a modified sugar precursor for sialic acid, they found azide group reactivity in highly purified RNA samples from the labeled cells (Flynn et al., 2021). Considering the extensive post transcription modifications RNA undergoes, the authors were motivated to investigate this the distribution of glycosylated RNA across the cell.

In order to test for distribution of glycosylated RNA, the researchers first used an enzyme named VC-Sia and tracked the dispossession of sialic acid on RNA molecules (Flynn et al., 2021).

This molecular scalpel, VC-Sia, precisely targets sialic acid and will snip it off molecules. Notably, VC-Sia can selectively remove these sugary tags specifically from the exterior of living cells. To track said dispossession of sugars from RNA, they utilized a metabolic label (Ac4ManNAz) incorporated into the sugar portion of glycoRNA transcripts (Flynn et al., 2021). After adding VC-Sia to living cell cultures, they observed a significant decrease in the amount of labeled glycoRNA only within 20 minutes (Flynn et al., 2021). This rapid digestion of glycoRNA indicates that the enzyme was able to access and modify a substantial amount of the glycoRNA. Remarkably, VC-Sia can selectively remove these sialic acid tags only from the outer surface of living cells, leaving the internal machinery untouched (Flynn et al., 2021). This implies that VC-Sia can access and alter a large fraction of glycoRNA in a short time frame, strongly hinting at glycoRNAs presence on the outer surface of living cells.

Building upon the initial findings with VC-Sia, the researchers sought to create an independent method to confirm the presence of glycoRNA on the cell surface. This new approach aimed to bypass the reliance on the original metabolic label (Ac4ManNAz), and to incorporate two different methods into one to achieve this (Flynn et al., 2021). The first method was a proximity labeling method that utilized peroxidase, an enzyme used to catalyze various oxidative reactions (Flynn et al., 2021). When the activation of Peroxidase occurs, it can create a highly reactive intermediate which can be used to tag nearby biomolecules. The researchers took advantage of this property by conjugating biotin-aniline, a molecule with strong affinity for RNA, to the peroxidase (Flynn et al., 2021). This ensured that when peroxidase was activated near RNA, the biotin-aniline would preferentially label the RNA. The second technique involved the strategic use of lectins, proteins that bind with carbohydrates (Flynn et al., 2021). By choosing

lectins with known binding specificities, the researchers could target the sugars accompanying glycoRNA. By combining both methods, the researchers were able to investigate the presence of surface-bound glycoRNA by labeling live cells with the lectin-peroxidase-biotin system (Flynn et al., 2021). Following labeling, they isolated the RNA from these cells to further analyze the pattern revealed by the labeling techniques. A distinct band from gel electrophoresis corresponding to high molecular weight RNA was specifically labeled only when cells were stained with MAAII and WGA (lectins that recognized sialic acid or N-glycans) (Flynn et al., 2021). Notably, ConA (a lectin that does not bind near glycoRNA acting as a negative control) did not produce this specific labeling (Flynn et al., 2021). This indicates that glycoRNA are in fact present on the cell surface in large quantities in certain cell types.

To solidify this observation, they treated the isolated RNA with an enzyme that will cleave cell surface RNAs from the cell membrane, RNase A. The resulting band displayed sensitivity to RNase treatment, further confirming its identity (Flynn et al., 2021). Additionally, treating the RNA with a sialidase enzyme, which cleaves sialic acid sugars, also resulted in displacement of the band in gel electrophoresis (Flynn et al., 2021). This suggested that sialic acid on glycoRNA contributes to its migration behavior in the gels used for analysis, further inferring that glycoRNAs are present on the cell membrane surface.

In conclusion, VC-Sia experiment was compelling for the presence of glycoRNA on the cell surface, and then the lectin-based labeling approach served as a powerful confirmation (Flynn et al., 2021). The rapid reduction in labeled glycoRNA during RNase treatments strongly suggested its outward projecting orientation on the cell membrane (Flynn et al., 2021). This research has paved way for development of this exciting new field in cellular biology, the world of cell-surface-

bound glycoRNA. The discovery of glycoRNA opens a discussion to the possibility of these glycoRNAs interacting with Siglecs. Siglecs, receptors found on immune cells, are known for their ability to bind sialic acid (Flynn et al., 2021). The possibility that specific Siglec proteins that act d· immune system regulators may bind to other cell types in the presence of glycoRNA may suggest glycoRNA has an important role in immune regulation (Flynn et al., 2021). Fueled by this possibility, research has sprouted from the findings of Bertozzi and Flynn which dive into the potential link between glycoRNAs and autoimmune diseases.

Key Takeaway: RNA has shown to act as a scaffold for sugars which has been termed as glycoRNA (Flynn et al., 2021). These glycoRNA exist within the cell and on the cell surface, making them a subtype of csRNA. Although glycoRNA is csRNA, not all csRNA is glycosylated. Methods in this paper use metabolic labeling of the sialic sugar attached to RNA, limiting the detection and profiling to glycoRNA. Methods to characterize non-glycosylated csRNA are needed. (Flynn et al., 2021)

iv. Spatial imaging of glycoRNA in single cells with ARPLA (2023):

GlycoRNAs have recently revealed themselves as a captivating area of research. However, studying these molecules and how they come to be present on the cell membrane has been proven as challenging. Existing methods lack certain details needed to fully grasp the properties and functions of glycosylated csRNA. This study introduces a novel approach, ARPLA (sialic acid aptamer and RNA in situ hybridization-mediated proximity ligation assay) which offers a powerful

tool for directly visualizing glycoRNAs on cells (Ma et al., 2023). This provides valuable insights of their spatial distribution on the cell membrane.

ARPLA works by leveraging aptamers to their advantage. Aptamers are short snippets of RNA engineered to bind specific targets. In the case of ARPLA, the designed aptamers will bind to the sialic acid modifications found widely on glycoRNAs (Ma et al., 2023). After the addition of the aptamer to the cells, a DNA probe is added specifically designed to hybridize to the exposed glycoRNA sequence (Ma et al., 2023; Tavoosidana et al., 2011; Yue et al., 2021). What is so special about the ARPLA system is its dual recognition. Both the aptamer targeting sialic acid and the DNA probe targeting an exposed glycoRNA sequence need to bind in proximity of each other for clear indication of glycoRNA on the cell membrane (Ma et al., 2023). This ensures high selectivity which significantly reduces the probability of false positives from detecting free aptamers or unrelated RNA molecules. Additionally, ARPLA boosts detection sensitivity. Once the aptamer and DNA probe come into proximity after recognizing their respective targets, a chain reaction is triggered. In situ ligation followed by rolling circle amplification (RCA) occurs (Ma et al., 2023). RCA is defined as the synthesis of nucleic acids on a circular template without stopping which leads to an increased number of RNA sites for further detection via fluorescent DNA probes (Ma et al., 2023; Söderberg et al., 2006). This amplifies the fluorescent signals marking the existence of glycoRNA on the cell surface even if their minimal expression .

After validating ARPLA's effectiveness in various cell models, the researchers used ARPLA to unveil subcellular distribution of glycoRNAs. They discovered a common colocalization with lipid rafts (an assembly of proteins and lipids free floating along the cell membrane) (Ma et al., 2023). Additionally, they observed distinct localization of glycoRNAs that provides evidence for their

involvement in secretory exocytosis, a cellular export process (Ma et al., 2023). Furthermore, the researchers utilized ARPLA to investigate glycoRNA abundance in breast cancer models. Interestingly, they revealed that a decrease in glycoRNA levels occurs as the cancer spreads. They also decided to look at immune cell models where they observed a reduction in glycoRNAs during cell maturation (Ma et al., 2023). Inversely they observed an increase of glycoRNAs during inflammatory responses. Furthermore, ARPLA provided evidence suggesting that glycoRNAs may play a crucial role in cell-cell interactions, specifically interactions between immune cells and blood vessel cells (Ma et al., 2023). These intercellular interactions could potentially influence inflammatory processes.

ARPLA represents a significant push in progress for the field of glycoRNA. The method's ability to visualize glycoRNAs with high sensitivity and selectivity provides a trustworthy means of tracking the expression of glycoRNAs through different cell types and disease states (Ma et al., 2023). Using ARPLA, scientists can now investigate deeper on of the roles glycoRNAs and how this newly discovered biomolecule contributes to various biological processes. It is worth mentioning that the methods used within this study are limited to visualization and detection of glycoRNAs and not non-glycosylated RNAs. Moreover, they cannot separate glycoRNA from the rest of the cell and profile the RNA sequences. The method is solely utilized for detection purposes.

<u>Key Takeaway:</u> Ma et al. was able to develop ARPLA, a new technique for detecting glycoRNA on different cell types. ARPLA stands for "sialic acid aptamer and RNA in situ hybridization-mediated proximity ligation assay" which requires both the sialic acid and matching RNA

transcript to be in close proximity of each other for the probes to recognize, bind, and activate the in-situ ligation for RCA to occur (Ma et al., 2023; Tavoosidana et al., 2011). This paper has developed a clever assay with higher sensitivity and selectivity to detect glycoRNA. However, since the assay relies on the presence of sialic acid for detection, it can only be used to detect glycoRNA and no other non-glycosylated csRNA types. (Ma et al., 2023).

v. Cell surface RNAs control neutrophil recruitment (2024):

Recent discoveries have unveiled a presence of RNA molecules adorning the outer surface of mammalian cells. Some of these surface RNAs are even modified with sugars. However, the true function and origin of these RNAs present on the cell surface remains a mystery. This study illuminates the true purpose of csRNAs, revealing a critical role in neutrophil recruitment (Zhang et al., 2024). This research encompasses the focus on neutrophil cell-cell interaction with endothelial cells. Neutrophils are known to be specialized white blood cells that act as the body's first responders to infections by promoting inflammation. This study discovered that cell surface RNA is essential for neutrophils to locate themselves to the site of infection (Zhang et al., 2024). This study also highlights the involvement of SID-1 protein, previously known for its role as a transporter of RNA across the cell (Zhang et al., 2024). Furthermore, by disrupting SID-1 homologs, they were able to effectively inhibit the production of glycoRNA in neutrophils (Zhang et al., 2024).

To investigate the function of glycoRNAs in neutrophils, they utilized a system where bone marrow progenitor cells from mice were immortalized, then induced to differentiate into neutrophils (Zhang et al., 2024). They then metabolically labeled these cells with molecule N-

azido-acetylmannosamine-tetraacylated via incorporation into the sialic acid synthesis pathway, the same method used by Flynn and Bertozzi in the glycoRNA article (Zhang et al., 2024). Again, this metabolic labeler tags the sialic acids on any glycoRNAs with a special azido group. This allows for the employment of click chemistry biotinylating of glycoRNAs after isolating total RNA from the labeled neutrophil cells. Biotin labeling showed a clear detection of glycoRNAs in neutrophils (Zhang et al., 2024).

Analysis of the purified RNA confirmed the presence of glycoRNAs due to biotin signals observed in both the immature and mature neutrophils. RNase A was used to create a negative control, which showed the depletion of glycoRNA biotin signaling after RNase treatment (Zhang et al., 2024). Supporting the data gathered from RNase used as a negative control, other enzymes like proteinase K, DNase I, or even RNase A pre-treated with an inhibitor did not affect biotin signals (Zhang et al., 2024). This strongly suggests that the signals are originated from genuine glycoRNA modifications and not from a contamination of DNA or proteins after isolating the RNA.

Furthermore, in gel electrophoresis the biotinylated RNA migrated slower than ribosomal RNA during electrophoresis, indicating a larger complex (Zhang et al., 2024). There was no background biotin signaling observed at the positions of major rRNA bands (28s and 18s) further ensuring the specificity of this detection method (Zhang et al., 2024). These experiments provided compelling evidence of the presence of glycoRNAs in neutrophils which paved the way for a more in-depth investigation of the functional role glycoRNA has on neutrophil cell membranes.

Having established the presence of glycoRNAs within neutrophils, next the researchers wanted to directly visualize RNA on the neutrophil's outer surface. To do this, they employed a

metabolic RNA labeler known as 5'-bromouridine (BrU) (Zhang et al., 2024). This BrU molecule essentially acts as a tag for RNA, very similar to Ac4ManNAz acting as a tag for sugars. Then, fluorescent antibodies specific to BrU could be applied to detect the presence of csRNA and imaged (Zhang et al., 2024). Initial attempts for visualization of csRNA were unsuccessful. They uncovered that cell surface glycoRNAs showed a resistance to RNase digestion compared to unmodified csRNAs (Zhang et al., 2024). This suggested a potential layer of protection provided to csRNA, capped or covered by unknown proteins that may be shielding csRNA, explaining the lack of accessibility for antibody detection. The researchers designed a new approach of briefly treating the BrU-labeled neutrophils with proteinase K (ProK) before adding the fluorescent anti-BrU antibody (Zhang et al., 2024). ProK is an enzyme that breaks down proteins, therefore removes the protective protein layer that is protecting csRNA. This ProK treatment allowed for the anti-BrU antibody to bind to the exposed BrU-tagged csRNA, showing fluorescent signal, and as expected, the resulting signals were eliminated by treatment with RNase A (Zhang et al., 2024). It is important to highlight that using antibodies to detect BrU are limited only to visualization and neutrophil localization studies. Since antibodies are proteins, they cannot utilize BrU to tag and separate the csRNA for sequencing. This is due to the harmful RNA isolation protocol necessary for separating RNA from total cell lysate. The non-covalent labeling of antibodies with BrU containing csRNA would be destroyed during this procedure. Despite this, the approach to visualize RNA on the cell surface solidified its presence on neutrophils.

The focus of their research quickly shifted towards investigating csRNA function in neutrophil recruitment to inflammation sites. In order to investigate this, they employed thioglycolate-induced peritonitis, a model that triggers inflammatory responses that attracts neutrophils

(Zhang et al., 2024). The researchers then developed a strategy to assess csRNA impact on recruiting neutrophils. Neutrophils were isolated from mice and separated them into two populations where each population was labeled with distinct fluorescent dyes (Zhang et al., 2024). One population received an enzyme treatment RNase A, cleaving external RNA molecules, while the other population remained untreated as a positive control (Zhang et al., 2024). Both neutrophil populations were then reapplied to the same mouse models of peritonitis via injection. After a short period, the researchers counted and compared the number of neutrophils from each population found within the inflammation site of the mouse model. Results showed that when comparing the control group to the RNase A treated group, there was a reduction of 9-fold observed with neutrophils lacking csRNA (Zhang et al., 2024). This suggests an important role for csRNA in recruiting neutrophils to sites of inflammation.

These in vivo experiments provide evidence that csRNA on neutrophils plays a crucial role in their recruitment to inflammatory sites. The results help pave the way for further exploration of the mechanisms involved in csRNA contribution to not only neutrophil function that influences the course of inflammatory disease, but additional csRNAs contribution to many other cell-signaling pathways found in different cell types.

Key Takeaway: This paper is one of the first to describe a function that csRNA has in a specific cell type. They confidently show that neutrophils not only present RNA on their cell surface, but without csRNA they lack recruitment to inflammatory sites (Zhang et al., 2024). This supports the hypothesis that csRNA is likely involved in cell adhesion correlated to immune response. In this study, they used a combination of Proteinase K and RNase A as well, which can be applied to

our experiments. Proteinase K cleaves extracellular proteins from cells to give antibodies (or in our case crosslinkers) better access to csRNA for higher binding efficiencies (Zhang et al., 2024). RNase A cleaves extracellular RNA, making this enzyme suitable for creating negative controls (stripping cell membranes of RNA)(Zhang et al., 2024). Additionally, this paper used BrU metabolic labeling for detection purposes. However, BrU nucleotide analogue can only be recognized by antibodies for detection, therefore is not suitable for isolation and profiling purposes. 4sU and covalent linkers should allow for the dual purpose of detection and profiling. (Zhang et al., 2024).

vi. Isolation of Newly Transcribed RNA Using the Metabolic Label 4-thiouridine (2018):

Understanding the creation, modifications, transformations, and degradation of RNA has been continuously studied to reveal the ultimate structures and functions of different types of RNA. Traditional methods have given insight on RNA specifications, however, they often come with limitations such as potential harm to cells and the lack of capturing the true dynamic of RNA in nature at a given time. To solve some of this limitation, a new chapter of next-generation sequencing technologies has provided a useful approach to couple with a metabolic labeling technique using a molecule called 4-thiouridine (4sU) (Garibaldi et al., 2017). This labeling technique has created the possibility to studying RNA dynamics over the whole genome with trustworthy accuracy and resolution.

4sU provides simplicity for tracking RNA from creation to degradation. By adding 4sU to mammalian cells, RNA polymerase will naturally incorporate the nucleotide analogue into the

RNA transcripts (Garibaldi et al., 2017). Because of this mechanism, scientists can metabolically label any newly synthesized RNA. Next, newly transcribed RNA tagged with 4sU can be isolated and analyzed by utilizing a crosslinker molecule using to gather data about the behavior of such RNA. Additionally, researchers can leverage 4sU to study RNA degradation. By replacing the cell culture media that contains 4sU with regular media after a certain period, they can collect data such as the half-life of the labeled RNA(Garibaldi et al., 2017).

After isolating total RNA from cell lysate, the unique chemical properties of 4sU can be exploited for crosslinking. The sulfhydryl group present on 4sU allows for its selective crosslinking of biotin molecules (Garibaldi et al., 2017). Utilizing biotin-streptavidin as a strong non-covalent interaction allows for the separation of newly labeled RNA from total RNA isolate. This 4sU labeled RNA separated from non-labeled RNA can be further analyzed by real-time PCR (qRT-PCR) or RNA sequencing (Garibaldi et al., 2017).

Given 4sU's ability to specifically mark nascent transcripts creates a great potential to study RNA biology. This methodology has paved the way for discoveries directly linked to changes in gene expression by studying RNA transcribed directly after genetic alteration. This allows for a deeper understanding of the involvement of RNA molecules in critical molecular cell mechanisms.

Key Takeaway: 4-thiouridine has previously been established as a good nucleotide analogue used to track RNA within cells. It has been used to study the synthesis, function, and degradation of different types of RNA (Garibaldi et al., 2017). The sulfhydryl group found on carbon 4 of the

uridine ring presents an opportunity for covalent labeling with click-chemistry, with limited disturbance on the cell's natural biological processes (Garibaldi et al., 2017).

vii. Tracking distinct RNA populations using efficient and reversible covalent chemistry (2015):

RNA dynamics within living mammalian cells are extremely significance for understanding gene regulation and various cellular processes. However, current methods for studying these dynamics often rely on antibodies to detect RNA. These antibody-based approaches have limitations, specifically the inability to isolate and profile RNA, prompting researchers to explore alternative strategies (Duffy et al., 2015).

The rationale behind the exploration of other strategies to label RNA is due to the drawbacks provided when using HPDP-biotin crosslinkers. This has been the universal method for labeling RNA molecules containing 4sU, and although effective, HPDP-biotin has limitations (Duffy et al., 2015). It exhibits a much lower crosslinking efficiency compared with other types of click-chemistry, resulting in a reduced yield of labeled RNA for analysis (Duffy et al., 2015). Also, HPDP-biotin forms a stable disulfide bond, making the labeling process irreversible which can be problematic for downstream applications that require the separation of RNA from the labeling tag to sequence the RNA (RNAseq of full transcripts rather than fragments) (Duffy et al., 2015). Length bias can also arise while using HPDP-biotin since longer RNA molecules naturally contain more uridine nucleotides compared to shorter ones, there are more opportunities for 4sU to be incorporated into longer fragments. This creates a bias of labeling when using HPDP due to a higher percentage of 4sU targets being on long RNA transcripts (Duffy et al., 2015). Therefore,

this preferential interaction leads to a skewed enrichment of longer RNAs due to their capture being more frequent. Although statistical corrections can partially address this issue, bias towards long non-coding RNA will alter results (Duffy et al., 2015).

MTSEA crosslinkers offer a compelling solution to these limitations. They boast a significantly higher crosslinking efficiency compared to HPDP-biotin and demonstrate a remarkable 2-fold increase in the yield of labeled RNA using MTSEA, improving the sensitivity of experiments (Duffy et al., 2015). The covalent bond created from MTSEA crosslinking is also reversible, meaning the disulfide bond created can be cleaved via a reducing agent (Duffy et al., 2015). This feature of MTSEA enables the separation of the RNA from a biotin tag for applications like RNA sequencing. Also, unlike HPDP-biotin, MTSEA-biotin appears to alleviate length bias. This advantage likely stems from the broader targeting mechanism MTSEA click chemistry provides, interacting with a wider range of functional groups within the RNA molecule (Duffy et al., 2015). Due to these MTSEA properties listed, plus the factor of MTSEA's impermeability, this crosslinker seems like a great tool for a non-biased technique for detecting, imaging, and profiling csRNA.

Key Takeaway: This article compares the crosslinking efficiency of previously used HPDP-biotin and MTSEA-biotin compounds. There are many advantages for using MTSEA over HPDP crosslinkers, especially for labeling csRNA. MTSEA is impermeable and the reaction time is significantly shorter than that of HPDP (Duffy et al., 2015). This is important for only crosslinking RNA on the cell surface and not intercellular RNA. Additionally, the crosslinking efficiency on modified RNA molecules has a much higher yield in MTSEA crosslinkers (Duffy et al., 2015).

Chapter 2:

Project Rationale:

The rationale behind this project is to utilize click-chemistry to label all types of csRNA. Other methods can either study glycoRNA or non-glycosylated RNA, or maybe a study only focuses on long non-coding RNA vs. shorter fragmented micro RNAs (Flynn et al., 2021; Huang et al., 2020; Lv et al., 2023; Ma et al., 2023; Zhang et al., 2024). There has yet to be a method that can label the wide range of csRNA despite their type. Additionally, previous methods have shown to be limited to only detecting csRNA or profiling csRNA, never both at the same time.

Using metabolic labeling techniques, such as the nucleotide analogue 4sU, in combination with MTSEA crosslinkers could solve this issue and provide a faster and more efficient approach to detecting and profiling csRNA in different cell types. There are many benefits of using MTSEA crosslinkers compared to previous methods:

- Quicker labeling times preventing disruption of natural cellular processes
- Non-specificity between glycosylated and non-glycosylated csRNA
- Impermeability allowing increased specificity towards csRNA over cellular RNA
- Covalency of click-chemistry providing retainment of the label during RNA isolation
- Reversibility of the reaction allowing for cleavage of crosslinker for sequencing

To research if MTSEA labeling of csRNA is in fact possible, the project flow is as follows (Figure 4). First, previously identified mammalian cell cultures that present csRNA (HELA & HEK293T) are metabolically labeled by 4sU and cultured overnight. The next day, the cell population is treated with MTSEA crosslinkers (either MTSEA-biotin or MTSEA-xx-biotin) followed by a series of intense washing to ensure no MTSEA products are left in solution during cell lysis.

During this step RNase A is used to treat the cells for development of a negative control, and Proteinase K is used to better expose the csRNA to the crosslinkers.

RNA isolation is then performed to separate total RNA from other cell components. These pure RNA samples can then be applied to a Dot Blot, a procedure used to immobilize RNA to a positively charged nylon membrane for ECL detection. Any signal from the Dot Blot indicates that csRNA is present within the sample, even though the blot is total RNA. Cells treated in-vitro with RNase A act as a negative control within this step and can be used to compare signals. The Dot Blot is an important checkpoint within the process of profiling csRNA for both detection purposes and labeling specificity.

Figure 4:

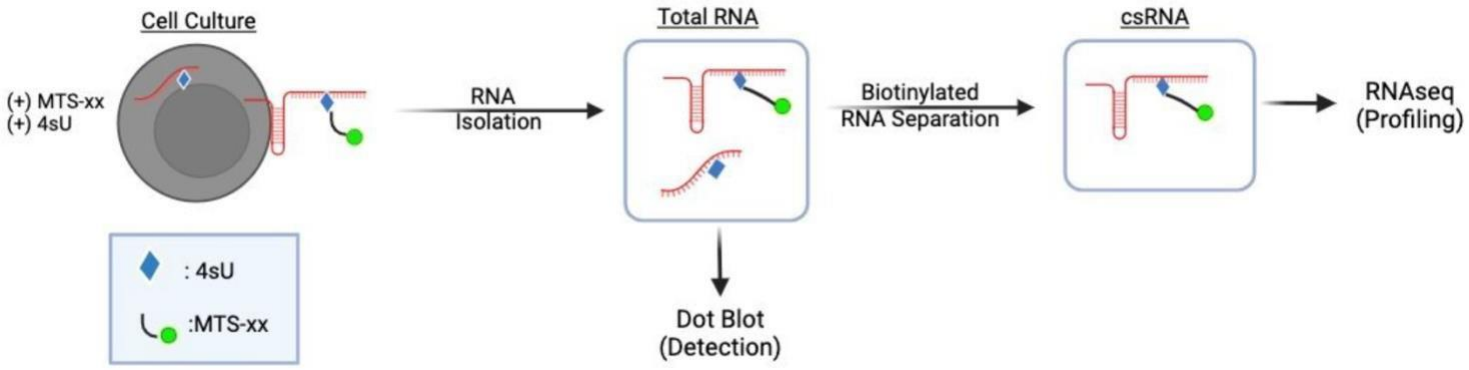

Fig. 4: Schematic representing project flow in accordance with the project rationale.

Total RNA samples with detectable csRNA via Dot Blot then undergo a 'Biotinylated RNA Separation' protocol. In this step, magnetic beads that are coated with streptavidin are incubated with the RNA samples. Since biotin and streptavidin have high affinity for one another, biotinylated RNA molecules will bind to these magnetic beads. The nature of the beads having a

magnetic property allows for separation of biotinylated RNA (csRNA) from the total RNA sample by a strong magnetic field. Elution of biotinylated samples can be performed via reducing agents such as DTT, which cleaves the crosslinker from the RNA making the csRNA readily available for sequencing directly after separation.

At first, Dot Blots for positive controls were inconsistent with a lot of background noise. In order to optimize the reliability of Dot Blot for detecting csRNA, 800 grit sandpaper was used to increase the absorbance rate of our blot samples into the nylon membrane. This resulted in a more defined detection when imaging. Using this process, we then were able to observe detection of csRNA with the MTS-xx-biotin crosslinker in comparison to the negative control. Reproducibility of detection is still being optimized, but there is a clear difference in intensity between the two samples at the same concentration. The streptavidin coated magnetic bead separation procedure has experienced a significant roadblock. There is currently no elution profile for positive control samples. Different eluting agents, including tris(2-carboxyethyl)phosphine (TCEP), Proteinase K, RNase A, and biotin, have been used at different pHs and temperatures. All agents used resulted in an elute RNA sample of minimal to none.

Methods/Materials:

I. Cell Culture:

Chemical crosslinking MTSEA compounds to csRNA were applied to mammalian cells that have previously been identified to express csRNA such as HeLa and HEK293T cell lines (Flynn et al., 2021; Huang et al., 2020). This section covers the protocols for the storage, release, and splitting of these mammalian cell lines to produce healthy cultures for treatment experiments.

- Cell Medium:
    - Growth Medium (GM): 10% Fetal Bovine Serum (FBS), 1% Penicillin-Streptomycin (PS), inside Dulbecco's Modified Eagle Medium (DMEM)
    - Cryo-storage Medium: 50% FBS, 40% DMEM, 10% DMSO (DMSO is added to help prevent ice crystal formation during the freezing process that would otherwise be harmful to the mammalian cells)

- Storage: Cell storage is the process of taking a live mammalian cell culture existing in natural growth medium and splitting it accordingly into cryo-medium contained inside cryo safe vials for storage at either -80° C or liquid nitrogen. The listed procedure below provides the steps needed to store mammalian cell culture.

    1. Remove medium from the cell dish
    2. Wash the cells with DPBS
    3. Detach the cells from the bottom of the plate by adding TrypLExpress (trypsin) (Gibco, Cat no.12604039) and let incubate at 37° C / 5% CO_2 (can check if cells are in suspended state underneath microscope)
    4. Quench the cells with growth medium at a ratio of 1:1
    5. Centrifuge at 600 x g for 3 minutes to pellet the cells

6. Resuspend the cells in Cryo-Medium and aliquot them into Cryo storage vials (1ml per vial) (If the plate being stored is full confluency, one plate can be split and stored into a maximum of 7 storage vials)
7. Freeze using isopropanol container inside -80° C before transferring to liquid nitrogen tank (isopropanol slows down freezing process of mammalian cells protecting them from harmful ice crystal formation)

- Release: Cell release is the process in which mammalian cell lines that are stored at -80° C or in liquid nitrogen are released back into their respective medium for proliferation in incubated cultures. The following listed procedure covers the protocol used to release cells back into culture.

1. Pre-warm growth medium in a water bath at 37° C
2. Thaw the culture vial by gentle agitation in a water bath at 37 C° (or whatever is considered the normal growth temperature for the specific cell line, normally 37° C)

- This step #2 is critical to ensure that as the mammalian cells thaw, ice crystals will not pierce the cells causing them to die. Thawing them quickly in the pre-heated water bath is essential to acquiring a healthy culture release with a proportion of more healthy cells than dead cells.

3. Remove the vial from the water bath and decontaminate it via 70% ethanol before putting it in the culture hood.
4. Transfer the contents to a sterile 15 ml centrifuge tube and add the previously warmed growth medium dropwise to a total of 10 ml.
5. Centrifuge the tube at 600 x g for 3 min to pellet the cells.
6. Vacuum off the supernatant and resuspend the cells in an appropriate volume of growth medium by pipetting up and down.
7. Transfer the content to a culture dish, add the appropriate volume of growth medium to fill the cell culture dish, label the dish, and place it inside a 37° C/5% CO_2 incubator.

- Splitting: Cell splitting is necessary once mammalian cell culture's confluency exceeds 100% of the culture dish. In other words, this means that the cells accompany the entirety of the culture dish and no longer have room to proliferate in a healthy state. If cells are not split, they may lose viability and the natural biomechanisms of the cell type may alter. Splitting normally consists of taking the cells and dividing them up into more plates giving the culture more space to grow. A detailed protocol with the general guidelines for cell splitting is as listed below.

1. Pre-warm growth medium in a water bath at 37° C
2. Discard the old growth media by vacuuming it off
3. Wash the cell with an appropriate volume of sterile DPBS (volume depending on plate size)
4. Add a volume of TrypLExpress (tryspin) that will cover the entirety of the plate
5. Place the culture dish inside the incubator for ~5 minutes to allow applied enzyme to detach the cells from the bottom of the plate
6. After the 5-minute incubation, observe if the cell are detached by microscope
7. Transfer the suspended cells to a 15ml or 50ml falcon tube and quench the cells by adding a 1:1 proportion of growth medium to the TrypLExpress suspension

    - Quenching the cells reapplies necessary nutrients needed for mammalian cell viability after exposure of harmful conditions such as trypsin.

8. Centrifuge at 600 x g for 3 minutes to pellet the cells.
9. Vacuum off the supernatant and resuspend the cells in growth medium.
10. Add resuspended cells back into cell culture dishes.

    - This is where splitting occurs, often utilizing more cell dishes than before, causing lower confluency per dish allowing them room to proliferate.

11. Fill up cell culture dishes to appropriate volume with growth medium, label the dish, and place inside 37° C/5% CO_2 incubator.

II. Metabolic Labeling RNA with 4-Thiouridine:

This is the process in which the nucleotide analogue, 4-Thiouridine (4sU) (Cayman Cat no.13957-31-8) is added to the mammalian cell culture and incubated for a period of time. This allows natural incorporation of the metabolic labels into RNA transcripts. This is essential for labeling csRNA. Mammalian cell culture should be around 60-80% confluency for adequate incorporation of 4sU.

1. Prepare 50mM 4sU suspension by adding 2.6mg of 4sU powder to 200ul of UltraPure water. The molecular weight of 4sU is 260.27, and depending on the final volume of medium, the weight and volume can be adjusted within proportion to the recipe above.
2. Final concentration of medium should be 150μM (range of 100-200μM is sufficient for labeling). To achieve this concentration, dilute 60μL of 50mM 4sU stock into 20mL of GM (depending on the total volume needed for treatment, the volumes can change as long as they stay proportional).
3. Vacuum off existing medium in the cell dish, wash with DPBS (remove DPBS), and add 4sU containing GM to the selected plates
4. Label plates as 4sU treated and place back into 37° C incubator overnight. Crosslinking treatment can be done the next day (some experiments require only 30min-4hrs of incubation time instead of overnight incubation).

III. MTSEA-biotin Crosslinking Treatment:

Crosslinking treatment of csRNA occurs the day directly after 4sU metabolic labeling. Overnight, the cells should have plenty of time to incorporate 4sU into the RNA transcripts and translocated the tagged RNA to the cell membrane, readily detectable . During this procedure, RNASE-A is used to create negative controls (Ma et al., 2023). This enzyme should cleave any extracellular RNAs exposed, developing a mammalian cell with no detectable csRNA. Additionally, Proteinase K (ProK) is used to cleave extracellular proteins as well (Ma et al., 2023). These membrane proteins have been speculated to cover or cap csRNA which could affect the availability of the 4sU sulfhydryl groups coming into close enough proximity to the crosslinker. By adding ProK, these proteins are digested revealing more of the RNA transcript. MTSEA-biotin crosslinkers are then added to the live cell culture for a short 10 min span to label csRNA.

- Prepare MTSEA-biotin aliquots (1mg/ml) from stock powder (Biotium, Cat no.90066) in dimethylformamide (DMF) beforehand (MTSEA-biotin stocks should be created fresh, shelf life of the compound is about 1-2 months once suspended in DMF)

- Create 100μM MTS solution by adding freshly made 1mg/ml stock solution to DPBS (763ul of MTS-biotin-xx stock into 20mL of PBS makes 100μM)
- Prepare RNASE-A (Thermo Scientific Cat no.R1253) at 1mg/ml from 10mg/ml stock solution
- Create 0.1 mg/ml RNASE-A concentration in DPBS
- Prepare Proteinase K from 5mg/ml stock, then further dilute the stock to a final concentration of 0.01 mg/mL in DPBS

1. Remove excess 4sU medium and wash cell cultures with DPBS
    - Wash 3 times with DPBS, 2 min between each wash, careful not to disrupt cells off bottom of plates
2. Add appropriate volume of 0.01mg/ml ProK (Thermo Scientific Cat no.EO0492) into the cell suspension and incubated at 37° C for 5 min
    - Wash once with DPBS, 2 min
    - After proteinase K incubation, cells will detach from bottom of the plate, therefore transferring the samples to a falcon tube and washing via centrifugation and resuspension is necessary after the following steps.
3. Add appropriate volume of 0.1mg/ml RNASE A into cell suspension, incubate 37° C for 15 min
    - Wash once with DPBS, 2 min
        i. Strictly for negative control samples, RNase A degrades extracellular RNAs
4. Add appropriate amount of 100μM MTSEA-biotin solution to the plates and incubate for 10min in the dark
    - Wash 3 times, 2min between each wash, do not disrupt cells (dropwise)
5. Scrape, or pipette off the remaining cell culture and centrifuge at 600 x g for 3 minutes to create cell pellet. Remove supernatant and store.

IV. RNA Isolation from Whole Cell Lysate:

The RNA isolation procedure separates out global RNA from the rest of the cell lysate. Using phase separation chemistry, three phases of the cell lysate are created (Garibaldi et al., 2017; Vennapusa et al., 2020).The bottom organic phase mainly contains proteins and lipids, the white strip interphase contains DNA, and the aqueous phase at the top holds all RNA. Listed below are the specific steps and reagents used to create this phase separation and furthermore precipitate the RNA, pellet the RNA, and resuspend the RNA in UltraPure water.

1. For each cell pellet add 1ml of TRIzol RNA isolator (InVitrogen, Cat no. 15596026) (if there is trouble lysing all of the cells, add an extra 1ml of RNA isolator and split lysis into two different tubes)
2. Add 1/5 volume of chloroform to the solution, mix vigorously and let sit at room temperature for 5 minutes. (Solution should turn into a milky-pink substance when mixed)
3. Centrifuge 12,000 x g for 15 minutes at 4° C
4. Transfer supernatant (aqueous phase containing RNA) to a new tube. Be careful to not accidently pipette out any DNA or other biomolecules from the organic layer.
5. Add an equal volume of isopropanol and 1μL of glycogen to the new tube (glycogen precipitates with RNA which allows for better visualization of the pellet after centrifuging.
6. Let the sample precipitate at -20° C for 30 minutes
7. Centrifuge 17,000 x g for 10 minutes at 4° C
8. At this step, the RNA pellet should be visible. Rinse the pellet with 1mL of 75% ethanol to get rid of contaminants and salts from the tube. Let sit for 3-5 minutes at room temperature.
9. Centrifuge to resolidify pellet, 17,000 x g for 5 minutes at 4° C
10. Discard ethanol supernatant and dry the RNA pellet for 2-5 minutes at room temperature. Use a chem wipe to cover the tube while the pellet is drying.
11. Add appropriate amount of UltraPure water to dissolve the RNA pellet, measure concentration via nano-drop, and store at -80° C

- Final volume of UltraPure water added to the RNA pellet may depend on what concentration of RNA is desired for downstream tests.

V. RNA Bleach Gel:

RNA bleach gels use the principle of gel electrophoresis to observe the integrity of RNA that has been isolated from mammalian cells (Aranda et al., 2012). A 2:1 ratio (28S:18S of rRNA) that can be distinctly observed at 4.5kb and 1.5kb respectively indicates that there is no RNase contamination that has degraded the RNA sample.

1. Create gel:
    - 1% w/v agarose in TAE Buffer (0.5g in 50ml)
    - 0.5% v/v bleach (250ul in 50ml), 5-minute incubation and swirl
2. Heat suspension in the microwave, 30 seconds twice and let cool between each
3. Add a single drop of Ethidium Bromide once the solution has cooled down to be able to touch the glass
4. Pour gel to mold
5. Load RNA samples and ladder to the gel lanes.
    - 5000 bp DNA ladder in the first lane.
    - Experimental samples all at the same concentration can be added to the next lanes as chosen. Add 1ul of loading dye to these samples to visualize the loading step.
6. Run gel at 100v for 35 minutes.
7. Use gel imager to take and save an image of the gel

VI. Development of Positive Controls:

Throughout troubleshooting these procedures for optimization, positive controls have been used to ensure functionality of these methods. These positive controls are created by crosslinking 4sU containing RNA after RNA isolation, therefore the MTSEA-biotin crosslinker will label total RNA rather than just csRNA which gives a much higher yield of biotinylated RNA sample (Figure 5)(Duffy et al., 2015; Garibaldi et al., 2017) . Below lists the contents of the reaction needed to create positive controls.

- Create MTSEA-biotin / 4sU RNA reaction cocktail (Table 1).
- Incubate and rotate in the dark for 10-20 minutes at room temperature
- Utilize RNA purification kit (InVitrogen Cat no.12183018A) to purify RNA from other cocktail components (centrifuges occur at 14,000 x g for 30 seconds unless specified otherwise):
    - I) Add 3:1 ratio of RNA Lysis Buffer to sample
    - II) Add an equal volume of 100% ethanol to the sample
    - III) Transfer the sample to the green spin filter, centrifuge, discard flow through
    - IV) Add 400 μL of RNA Prep Buffer, centrifuge, discard flow through
    - V) Add 700 μL of RNA Wash Buffer, centrifuge, discard flow through
    - VI) Add 400 μL of RNA Wash Buffer, centrifuge for 1 minute, discard flow through
    - VII) Carefully take spin filter and transfer it to a new 1.5 mL tube for collection
    - VIII) Add 50-100 μL of UltraPure water to the center of the filter, centrifuge, collect flow through.
    - IX) Measure concentration of positive control, crosslinked RNA via nano drop and store sample at -80 °C

Figure 5:

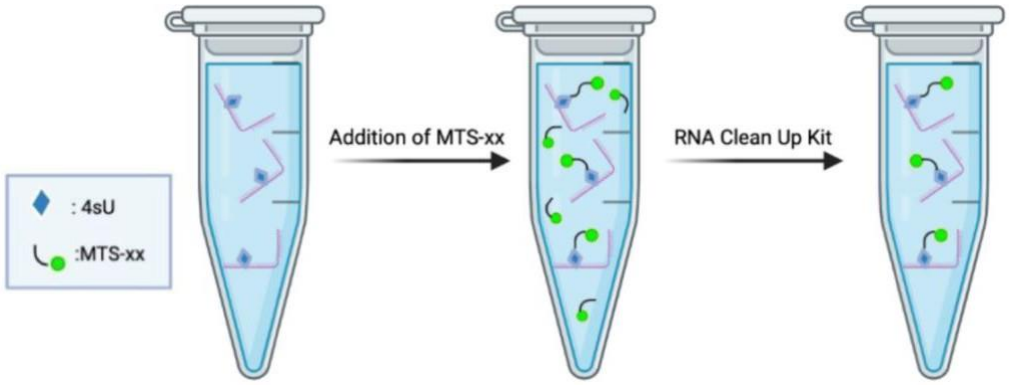

Fig. 5: Visual representation of using the same MTSEA crosslinking click-chemistry mechanism to create a positive control sample, occurring within a tube after cell lysis, labeling total RNA.

Table 1:

Components	Volume
RNase-free water	344 µl
1 M Tris–HCl (pH 7.4)	5 µl
0.5 M EDTA	1 µl
1 µg/µl 4sU labeled total RNA	50 µl
1 mg/ml MTS-biotin-xx	100 µl (must be added last)
Total volume	500 µl

Table 1: MTSEA-biotin + 4sU labeled RNA crosslinking reaction cocktail

VII. Detection of Biotinylated RNA via Dot Blot Assay:

The dot blot assay is a means to immobilize RNA samples on a positively charged membrane for a subsequent set of blocking, streptavidin-HRP treatment, washes, and Enhanced Chemiluminescent detection (ECL detection) (Figure 6) (Ren et al., 2018)This method allows for the detection of csRNA even before being separated from total RNA. RNase A treated cell cultures will be used as negative controls during this protocol.

1. Create Dot Blot buffers:
    - Blocking buffer: 10% SDS, 1mM EDTA, dissolved in PBS (pH 7.5)
    - Washing buffer #1: 10% SDS, dissolved in PBS (pH 7.5)
    - Washing buffer #2: 1% SDS, dissolved in PBS (pH 7.5)
    - Washing buffer #3: 0.1% SDS, dissolved in PBS (pH 7.5)

2. Develop a Dot Blot "map" showing which samples represent which blot and their concentrations.
3. Use fine sandpaper (DuraGold, Cat no. DUR WD-800) to eliminate the non-absorbent cover associated with the nylon membranes. This allows for better dissolving of the samples after blotting.
4. Add RNA samples to the nylon membrane according to the previously made map. Add anywhere between 2 μL and 10 μL of sample to the membrane.
5. After blots are fully dried, UV crosslink the membrane. This step non-specifically will covalently bind all single stranded RNA molecules to the positively charged membrane, so they are not washed off in the following washing steps.
6. Incubate the membrane in the blocking buffer for 20 minutes on a plate shaker
7. Remove blocking buffer and add new blocking buffer containing a 1:10,000 dilution of 1mg/ml strep-hrp (thermo-fisher).
8. Wash membranes with the following wash buffers
    I) Wash twice with buffer 1, 10 minutes each
    II) Wash twice with buffer 2, 10 minutes each
    III) Wash twice with buffer 3, 10 minutes each
9. After the last wash, dry the membrane on a chemiwipe until there is no visible pooling of wash buffer on the top of the membrane.
10. Transfer the membrane to a transparent plastic cover and add an adequate volume of ECL detection reagent.

11. Use a chemiluminescent imager to capture and visualize blot detection indicating the presence of biotinylated molecules.

Figure 6:

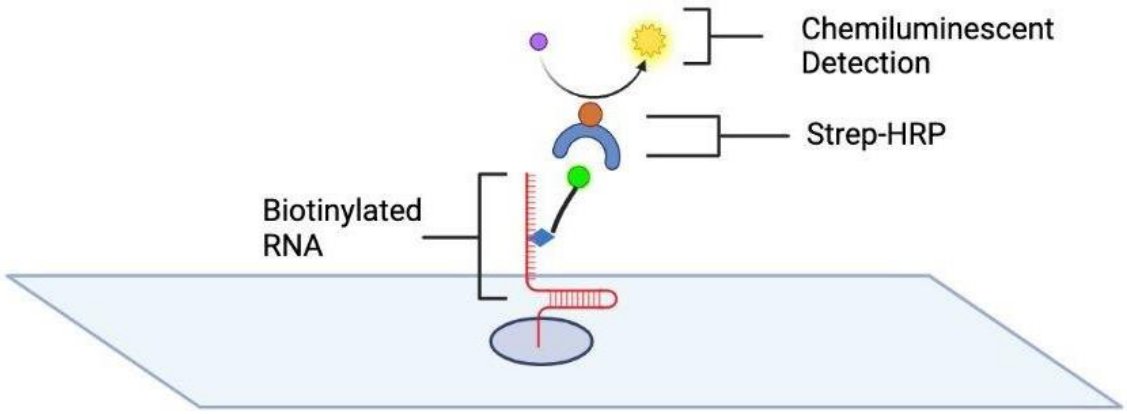

Fig. 6: Dot blot rationale. Immobilize biotinylated RNA for addition of strep-HRP and ECL detection reagents.

VIII. uMACS RNA Separation:

This separation procedure is to further biotinylated RNA molecules from a total RNA sample. This is necessary for further RNA sequencing to occur with pure csRNA. The magnetic beads (Miltenyi Biotec, Cat no.130-133-282) used are coated with streptavidin, therefore biotin molecules will bind tightly to the magnetic beads followed by a set of washes that will rid the sample of non-biotinylated molecules (Figure 7) (Garibaldi et al., 2017; Xu et al., 2017). Due to the specific nature of MTSEA-biotin crosslinkers making di-sulfide bonds with 4sU, in principle the biotinylated RNA can then be eluted off of the magnetic beads using a reducing agent such as DTT or TCEP .

1. Use 100 μL of biotinylated RNA for each uMACS column (Miltenyi Biotec, Cat no.130-133-282) at a suggested concentration of 450-500 ng/μL.
2. Add 100 μL of UltraPure water to reach a final volume of 200 μL.
3. Denature the RNA samples at 65°C for 10 minutes, followed by rapid cooling on ice for 5 minutes.
4. Add 200 μL of streptavidin coated beads and mix/rotate for 15 minutes at room temperature.
5. During the 15 minutes of incubation, warm nucleic acid equilibration buffer to room temperature and prepare columns by rinsing them twice with 100 μL of the nucleic acid equilibration buffer.
6. Prepare elution buffers:
    - 100 mM Dithiothreitol (DTT)
    - 100 mM Tris(2-carboxyethyl)phosphine (TCEP)
    - 25 mM Biotin (solution needs to be heated up to 95°C to dissolve biotin)
    - 1 mg/mL Proteinase K
    - 100 μg/mL RNase A
7. After incubation is finished, spin down RNA/bead samples and gently resuspend. Add total volume of loading sample to the respective column.
8. Spin down “flow RNA” and reload into columns for 2 extra cycles. Collect and label flow RNA sample.
9. Wash column with 200 μL of 55°C washing buffer. Collect this flow inside of the same “flow RNA” tube. Continue to wash the column for an additional two times with 55°C washing buffer. These flow throughs do not need to be collected.
10. Change the collection tubes to a new tube labeled “Elute RNA” and add 100 μL of elution buffer (DTT, TCEP, RNase A, ProK, Biotin). Allow for incubation of 5 minutes each before adding elution buffer again two more times. The total elution incubation should be three and total “Elute RNA” volume is 300 μL. Parafilm can be used to cap the bottom of these columns to retain the elution buffer. Incubation time and temperature of during elution can be altered accordingly depending on type of elution.
11. Recover the Flow and Elute RNA via RNA Isolator Kit as described in “Development of Positive Control” protocol.
12. Measure the concentration of “Flow RNA” and “Elute RNA” via nano drop.
13. % yield calculations can be done by dividing the Flow RNA and Elute RNA samples by the total RNA input recorded at the beginning.

Figure 7:

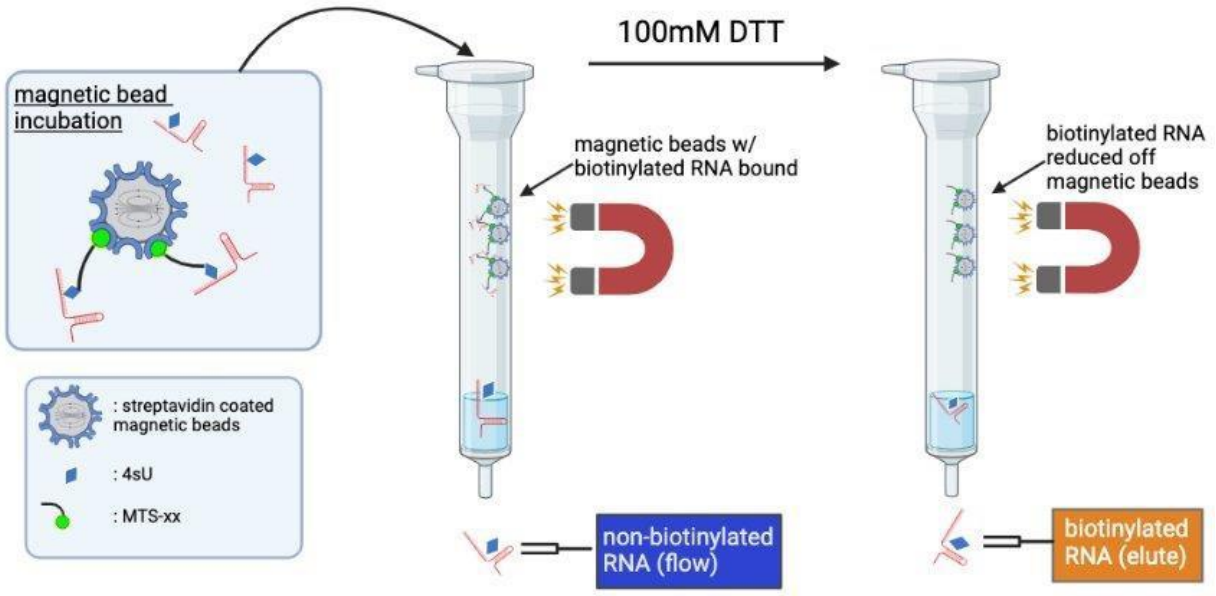

Fig. 7: uMACS biotinylated RNA separation schematic. Addition of magnetic bead/biotinylated RNA mixture to uMACS columns and magnet allows for subsequent washings and elutions resulting in separation of biotinylated RNA from non-biotinylated RNA.

IX. DynaBead RNA Separation:

Due to some elution issues with the uMACS separation procedure, a different type of streptavidin coated bead separation was explored named DynaBead RNA Separation (InVitrogen Cat no. 11205D) (Tsuji, 2023; Xu et al., 2017). This type of separation does not occur within a column, but instead within Lo-Bind tubes that can be regularly taken off the magnet to resuspend the beads in buffers. Specifically, it was decided to use this separation method to see if resuspending and aggregating the magnetic beads in our elution buffers would allow for a higher "Elute RNA" sample yield.

- High salt washing buffer 10x
    - 100mM Tris-HCl, pH 7.5
    - 10mM EDTA
    - 1M NaCl
    - Add 0.05% Tween-20 fresh to 1x aliquoted solutions fresh on day of separation

- Elution Buffer
    - 100mM DTT, added fresh on day of separation
    - 20mM HEPES, pH 7.4
    - 1mM EDTA
    - 100mM NaCl
    - 0.05% Tween, added fresh on day of separation

- Bead Blocking Buffer
    - 1x high salt wash buffer

40 ng/ µl glycogen

<u>Pre-Wash Dynabeads™ MyOne™ magnetic beads</u>

- First calculate the number of beads required based on their binding capacity (see Table 2 of DynaBead manual), and transfer the beads to a new tube (about 50ul beads per + control sample [70ng/ µl in 50ul])

1. Resuspend the beads in the vial (i.e., vortex for >30 sec, or tilt and rotate for 5 min).
2. Transfer the desired volume of beads to a tube. Wash with NF water 2 times.
3. Add 500ul of High Salt WB 1x and resuspend. Place the tube on a magnet for 1 min and discard the supernatant. Repeat once.
4. Add 1ml freshly made Bead Blocking Buffer, resuspend, and incubate for 1h at room temperature. Place the tube on a magnet for 1 min and discard the supernatant.
5. Add 500ul of High Salt WB 1x and resuspend. Place the tube on a magnet for 1 min and discard the supernatant. Repeat once.

Immobilize nucleic acids: Coating beads with RNA samples, Washing, and Eluting

1. Add the previously calculated volume of biotinylated DNA or RNA to the washed beads. Add appropriate amount of High Salt WB 1x to the RNA sample to make it at least 100ul.
2. Incubate for 15 min at room temperature using gentle rotation.
3. Separate the biotinylated DNA or RNA coated beads with a magnet for 2–3 min.
4. Wash the coated beads 2–3 times with High Salt WB 1x
5. Collect the wash flow for Qbit/Tapestation/RNAseq testing
6. Add 200ul freshly made elution buffer to the beads, mix the beads by inversion, wrap the tubes in foil, and incubate them at room temperature in the dark for 15 min
7. Quickly spin down the tubes and capture the beads in a magnetic rack for 2 min. Carefully retrieve the supernatant with a pipette and save this sample as “elution”.
8. Repeat step 7 with another 200ul elution buffer and immediately place tubes magnetic rack for 2 min. Remove the supernatant with a pipette and combine this elution with the previous elution samples.
9. Measure “Flow RNA” and “Elute RNA” via nano drop.

X. Qbit RNA Concentration Quantifications:

The Qbit protocol for measuring the concentration of RNA works in a different manor than nano drop (InVitrogen Cat no. Q33238) (Li et al., 2015a) In this method, RNA samples are combined with a working solution with fluorescent dyes very specific to RNA molecules. The instrument measures this fluorescent signal rather than measuring absorbance at 280nm like in the nano drop instrument. This allows for a more accurate concentration prediction given by Qbit machine (InVitrogen Cat no. Q33238) and allows for a better sensitivity at much lower RNA concentrations (Li et al., 2015b). Additionally, there are working solution buffers that measure microRNA, small snippets of RNA, which is possibly what csRNA is consisted of.

- Preparing samples and standards (all materials and reagents must be at room temperature)

1. Set up the required number of Qubit™ tubes (Invitrogen Cat no. Q32856) for standards and samples. The Qubit™ RNA HS assay (Invitrogen Cat no. Q32852) requires 2 standards
2. Label the tube lids accordingly
3. Prepare the Qubit™ working solution by diluting the Qubit™ RNA HS reagent 1:200 in Qubit™ RNA HS buffer. Use a clean plastic tube each time you prepare Qubit™ working solution.
4. Add Qubit working solution to each tube such that the final volume is 200 microliters
5. Add 10 microliters of each qubit standard to the appropriate tube
6. Add 1-20 microliters of each user sample to the appropriate tube
7. Vortex for 3-5 seconds and allow all tubes to incubate at room temperature for 2 minutes.

- Reading standards and samples

1. On the Home screen, touch RNA, then select RNA High Sensitivity as the assay type. Touch Read standards to proceed
2. Insert the tube containing Standard #1 into the sample chamber, close the lid, then touch Read standard. When the reading is complete (~3 seconds), remove Standard #1
3. Insert the tube containing Standard #2 into the sample chamber, close the lid, then touch Read standard. When the reading is complete, remove Standard #2.
4. Touch Run samples.
5. On the assay screen, select the Sample volume and units.
6. Touch the + or – buttons on the wheel, or anywhere on the wheel itself, to select the sample volume added to the assay tube (1–20 µL).
7. From the Unit dropdown menu, select the units for the output sample concentration
8. Insert a sample tube into the sample chamber, close the lid, then touch. Read tube. When the reading is complete (~3 seconds), remove the sample tube. The top value (in large font) is the concentration of the original sample, and the bottom value is the dilution concentration
9. Repeat step 6 until all samples have been read.

XI. Ultra-Performance Liquid Chromatography:

Ultra-high performance liquid chromatography (UHPLC) separates the components of a mixture based on their differing interactions with a stationary phase and a mobile phase, each moving at different rates depending on their polarity and affinity for the stationary phase (Lewis et al., 2016). Ultra-Performance Liquid Chromatography (UPLC) was utilized to confirm the chemistry of crosslinking molecules such as MTSEA-biotin and 4sU. It also was used to confirm the reduction chemistry reaction using DTT to separate MTSEA-biotin from 4sU (Figure 8). Throughout this method, only 4sU monomers can be used, for RNA cannot be put through the machine. These reactions were performed by simply adding an equal molarity of the 4sU monomer to the MTSEA-Biotin compound for crosslinking. 100mM of DTT was then used to reduce this reaction in a separate sample and was ran through the instrument as well. The mobile phase used was a gradient of methanol and water with minimal amounts of acid for pH stability. Detection of the molecules in the samples ran were done via mass spectrometry, fed directly after reverse phase separation. For reference, the molecular weights of each compound fed through the UPLC are as follows: 4sU = 260 g/mole, MTS-xx = 607 g/mole, crosslinked product = 787 g/mole (Figure 8).

Figure 8:

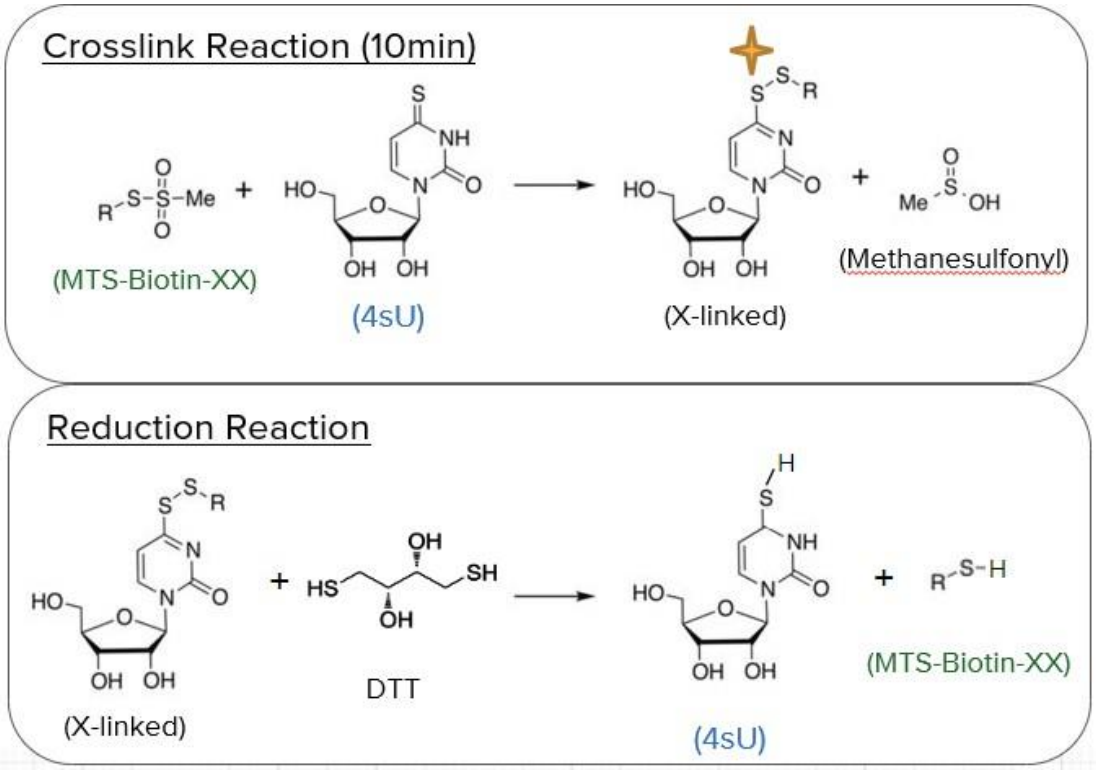

Fig. 8: Compounds MTSEA-xx-biotin and 4sU crosslinking reaction. This reaction results in a loss of a methane sulfonyl. The reduction reaction induced by DTT cleaves the di-sulfide bond resulting in the 4sU monomer and MTSEA-xx-biotin to separate. MTSEA-xx-biotin molecular weight after crosslinking is ~527 g/mole due to the loss of methane sulfonyl.

Chapter 3:

Results:

1. Developing csRNA Detection Methods Using 4sU Labeling and MTSEA Crosslinking Techniques

1.1. Dot Blot Optimization: Developing Reproducible Results with New Nylon Membranes

The first attempts at using positive controls to confirm the Dot Blot protocol were not as clean as anticipated following protocols I, II, VI, & VII from the methods section. The positively charged nylon membranes used were from Roche (Cat.# 11209299001), instead of the membranes previously used for RNA-biotinylating detection. These membranes seemed to have a protective coating on them, preventing the absorbance of RNA onto the blot. This resulted in a significant increase in blot absorbance time to be about 2 hours of drying before the UV crosslinking step. Additionally, the imaging of the membrane via ECL detection showed an abundance of background noise and unclear/hollow blots where samples were placed (Figure 9).

Figure 9:

1) 1,341 ng/µl

2) 134 ng/µl

3) 13 ng/µl

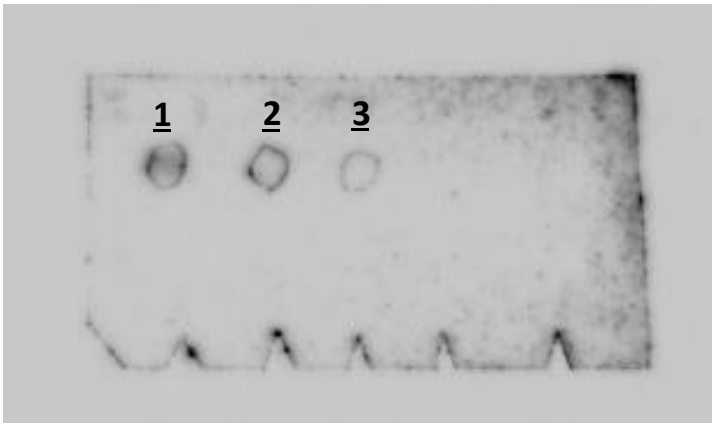

Fig. 9: Initial Dot Blot trial with positive control, serial titration to test sensitivity. Starting at 1,341 ng/µl followed by a 10% dilution for subsequent blots.

Due to these initial results, optimization of the dot blot method was necessary for applying in the detection of csRNA. The Roche Nylon Membrane product information sheet mentions that these membranes do not need to be pre-wetted and dried before application of the sample, however, it is generally recommended for clearer blots. Accordingly, we decided to try this method of pre-wetting the membrane to see if absorbance time would decrease and background noise seen around the edge of the membranes would disappear. Pre-wetting the membrane for 30 minutes before adding the sample resulted in a cleaner more distinct dot blot signal for the positive controls, however, there still existed significant background signal found on the outside border of the membrane (Figure 10).

Figure 10:

1) 300 ng/µl

2) 30 ng/µl

3) 3 ng/µl

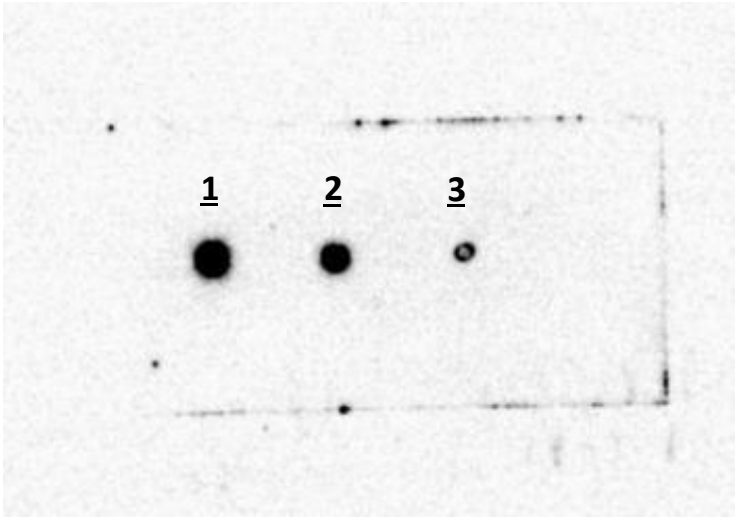

Fig. 10: Pre-wetted membrane positive control. Starting at 300 ng/µl and then serial titrating it twice for a 10% and 1% sample.

Additionally, within the Roche membrane product sheet, they mentioned the use of a vacuum apparatus that helps pull blots down into the membrane, assisting in blot sample

absorbance (*Nylm-Ro*, n.d.). However, a vacuum apparatus specifically designed for dot blotting are upwards of $2,000 which goes against the goal of this study; to create an affordable and easy protocol for detection and profiling csRNA. Therefore, we decided to create one. We made one by taking a buffer filter system and removing the filter paper that was lining the circular bottom (Figure 11). The filter system has a valve that can be hooked up to a vacuum, providing suction of the blotted sample into the membrane. Using this makeshift vacuum apparatus did in fact show distinct positive control sample detections and eliminated background noise previously observed on the outer edges of the membrane (Figure 11).

Figure 11:

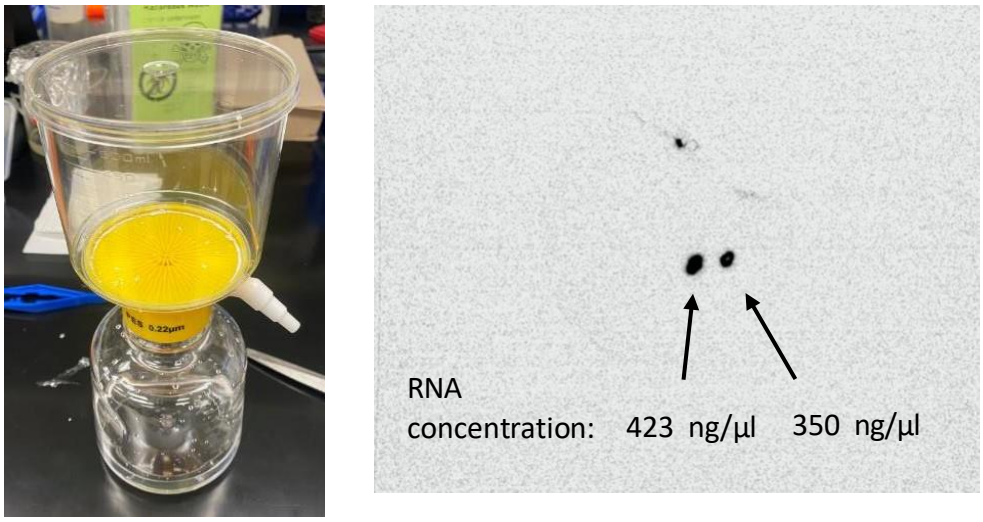

Fig. 11: Detection of two positive controls (experimental duplicates) via Dot Blot. Vacuum apparatus shown on the left, used for pre-wetting the membrane and absorbing blots into the membrane.

However, the method was extensive and tedious. Even after pre-wetting the membrane, the vacuum did not seem to increase the absorbance rate of the samples, resulting in ~ 1 hr of wait time before the UV crosslinking step. Additionally, for the vacuum apparatus to achieve

optimal suction, the membrane must be precisely cut to fit the circular bottom of the apparatus. If the membrane is not the right shape, air holes on the sides will eliminate any suction force through the membrane. Therefore, a better solution for optimizing the dot blot procedure by decreasing the time it takes for absorbance and eliminating background noise was necessary.

Due to the previous observations of the nylon membrane having a slick, hydrophobic coating on them allowed us to come up with a hypothesis that by somehow removing this coating we could achieve a faster absorbance rate. To do so, fine 800 grit sandpaper was used to sand down this coating. It was immediately apparent that the subsequent blotted samples were absorbing at a much faster rate, even without pre-wetting the membrane. Additionally, this method provided very limited background noise and nearly eliminated any signals observed on the outer portion of the membrane (Figure 12). It is important to mention that up to now, 1 hr of cross-linking incubation was used to develop positive controls (Figure 12). This was just to ensure that crosslinking was occurring at high efficiency and does not represent the crosslinking time of 10-20 minutes that is performed in-vitro on mammalian cell culture (csRNA labeling). At this stage, we were able to achieve a clear detection with lower limit of detection of ~3ng/μl. Sensitivity of this assay is very important for csRNA detection, because csRNA is likely a very small percentage of total RNA. Labeled csRNA sample concentrations represents total RNA concentration, not csRNA alone.

Figure 12:

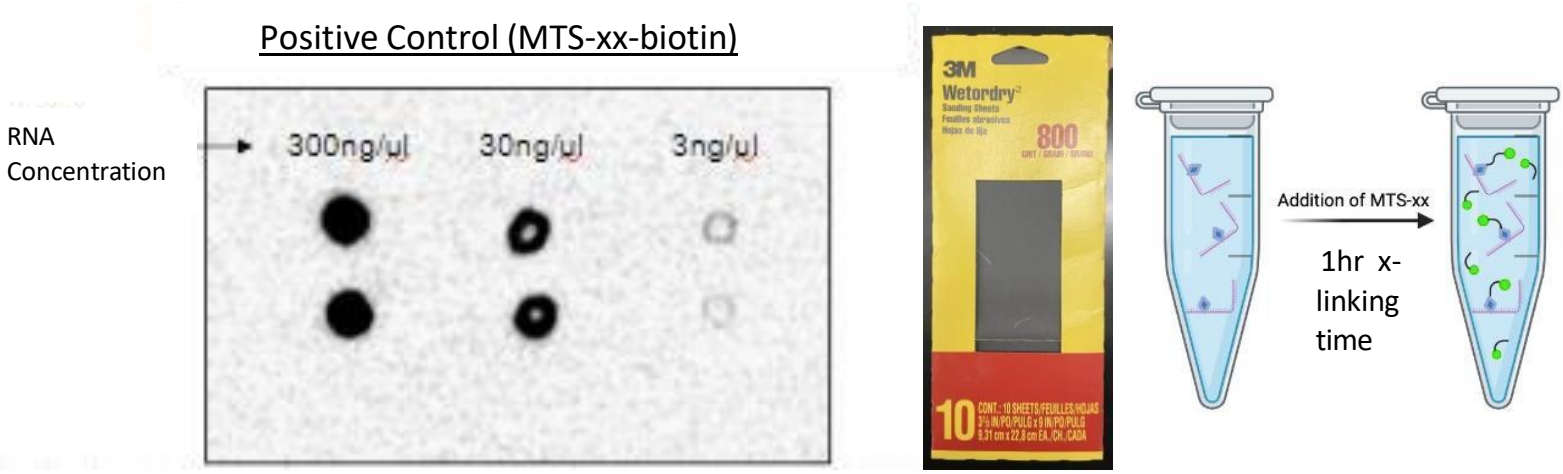

Fig. 12: Positive control Dot Blot (technical duplicates), using 800 grit sandpaper to increase absorption rate of sample which displayed a decrease in background noise.

1.2. Confirming Crosslinking Time Efficiency

Using the newly optimized Dot Blot protocol, it seemed necessary to ensure that a 10–20-minute crosslinking incubation was enough time to visualize a signal via ECL detection. Previously, we used an hour incubation to ensure a high yield of crosslinking. However, the crosslinking time performed in mammalian cell culture must be 10-20 minutes to ensure that no crosslinker is getting into the cell and being exposed to intercellular RNAs. This may yield false positives. Therefore, we tested a 10- and 20-minute crosslinking incubation time and performed the Dot Blot. It was clear that 10-20 minutes is sufficient for MTSEA-xx-biotin to crosslink with 4sU containing RNA. Furthermore, the sensitivity (down to 1.6ng/µl) was observed to be similar with this crosslinking time vs. the 1-hour incubation (Figure 13). This demonstrated that the incubation of 10 minutes for in-vitro crosslinking of csRNA will be sufficient to biotinylate csRNA for detection.

Figure 13:

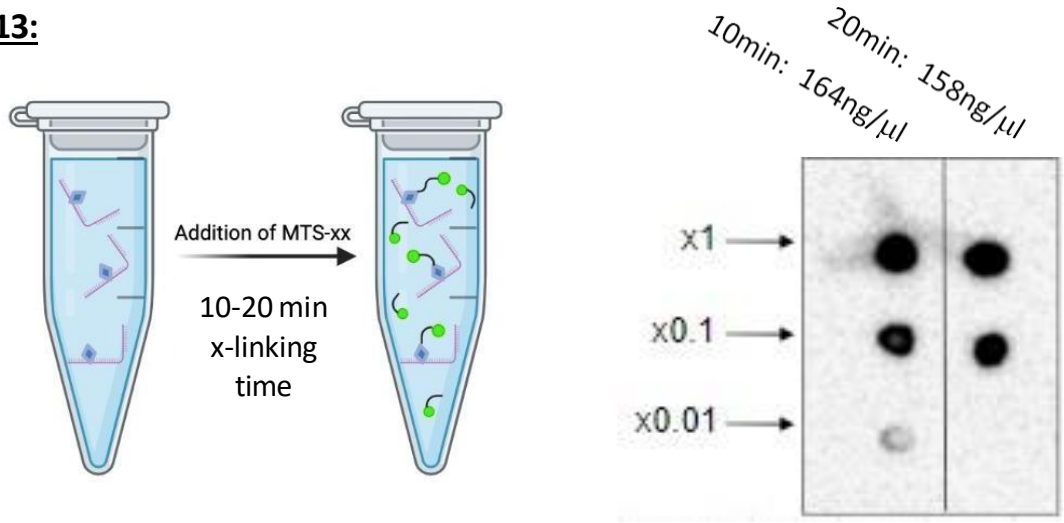

Fig. 13: Confirmation that a 10–20-minute reaction time for MTSEA click chemistry is optimal for creating positive controls, directly representing the time of in-vitro crosslinking incubation.

1.3. csRNA Detection

Now that the Dot Blot has been optimized and positive control sample detections are reproducible, we applied this method on detecting MTSEA-biotin crosslinked csRNA from mammalian cell cultures. The rationale here is to have a negative control where the mammalian cells are treated with RNase A before addition of a crosslinking agent. Therefore, by comparing the Dot Blot detection of csRNA to the RNase A (-) blot, we can confidently indicate whether csRNA was crosslinked with the MTSEA agents. One of the first successful indications of csRNA detection via Dot Blot is represented in Figure 14. Notice how the same sized sample was blotted on the nylon membrane at a similar concentration for direct comparison. Although the signal is faint, a very clear difference in signal between the csRNA detection and RNase A (-) control is shown.

Figure 14:

1) 3.8 ug/µl (csRNA)

2) 3.5 ug/µl RNase A Treated

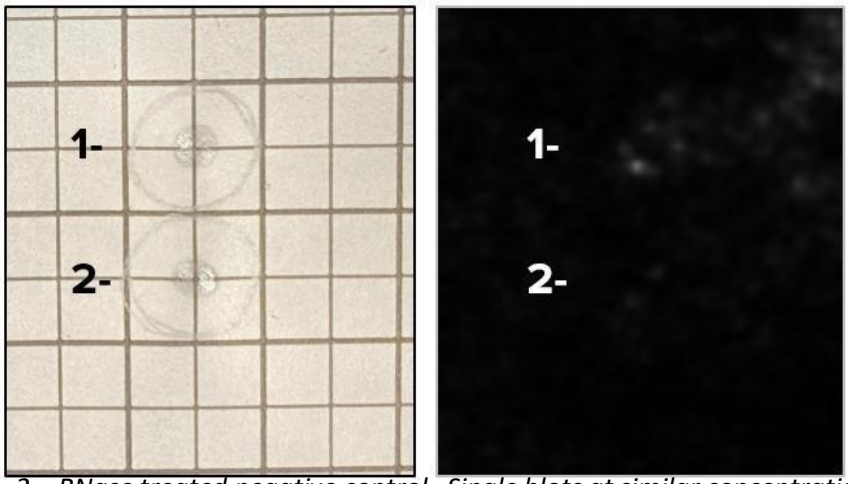

Fig. 14: 1 – labeled csRNA, 2 – RNase treated negative control. Single blots at similar concentrations showed a faint but clear difference in signal comparing csRNA to negative control.

At this point, the reproducibility of this result was difficult to achieve due to a general decrease in total RNA concentrations. Although the detection at ~3.5 ug/µl showed good results, the majority of samples gathered and tested on the Dot Blot ranged from 0.5 – 3.0 ug/µl. Even though this is a relatively high concentration resulting from the RNA isolation procedure, it may be too low for detection csRNA due to the increased probability of this type of RNA being such a low percentage of total RNA. Therefore, we aimed to increase the total cell culture volume and decrease the final water volume of isolated RNA. In combination, this was able to increase the total concentration of isolated RNA samples like the successful detection in Figure 14. Additionally, in attempt to increase the sensitivity of detecting csRNA, the total exposure time during imaging was manually increased as well. This is simply the amount of time the camera is exposed to the light produced by ECL agents which can result in a more defined detection image. Together, these changes resulted in the detection found in Figure 15.

Figure 15:

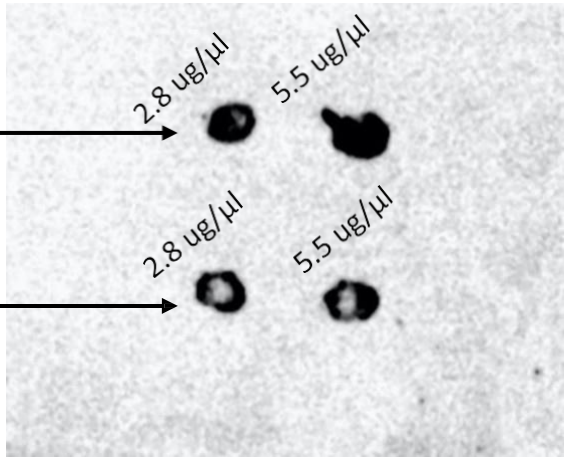

Fig. 15: Dot Blot detection of csRNA compared with RNase negative control counterpart. Clear difference between the experimental duplicates representing a stronger detection in csRNA vs. RNase treated samples at the same concentrations.

As represented in Figure 15, the csRNA samples seem to show a more intense detection compared to the RNase A (-) counterpart. This gives confidence that the MTSEA-xx-biotin crosslinker is in fact binding to csRNA. However, it is of concern that there is still signal being shown in the RNase A (-) sample. This could be a result of a few different things. First, it could mean that the MTSEA-xx-biotin crosslinker is impermeable, which seems unlikely due to the chemical's structure and what is known about selective permeability in mammalian cells. Second, it could be that the RNase A incubation on the mammalian cell culture is not optimal which may leave some csRNA still intact and readily available for crosslinking in the negative control samples. Lastly, it could mean that at some point the MTSEA-xx-biotin crosslinker is encountering lysed or dead cells. This could be a product of the mammalian cell culture viability not being optimal, or the washes after crosslinker incubation is not fully purging non-crosslinked MTSEA-xx-biotin from the mammalian cells. This would expose intercellular 4sU labeled RNA to

the crosslinker during the RNA isolation procedure, causing the detection we see from our RNase A (-) control.

2. Developing Magnetic Bead csRNA Separation Procedure: Troubleshooting Positive Controls for Elution Optimization

2.1. Magnetically Separating Biotinylated RNA from Non-Biotinylated RNA

The uMACS separation protocol is another method that needed to be optimized by using positive control samples. Practically, uMACS separation should provide quantitative data for csRNA abundance in a specific cell culture size. It also may indicate the percentage of csRNA compared to total RNA by comparing the eluted sample from flow sample. An initial trial of uMACS separation, using DTT as the di-sulfide reducing agent for elution, is represented by Figure 16. .Four different samples were used in this trial: MTS-xx-biotin labeled csRNA, RNase A (-) treated sample, positive control sample (4sU+MTS-xx), and ssDNA (+). The DNA sample was used as a second positive control which was purchased already biotinylated. It is important to understand that the biotinylated ssDNA (+) is not expected to elute, because there is no disulfide bond linking the nucleotides to a biotin molecule. The ssDNA (+) is a control to ensure that biotinylated molecules are in fact binding to the streptavidin coated beads. The major issue is that the 100mM DTT elution buffer does not seem to be successfully eluting the biotinylated RNA from the column. This is clearly an issue that blocks the collection and sequencing of biotinylated RNA after separation. However, it is possible to still compare where most of the RNA resides after the procedure. The trend of biotinylated nucleotides found either in the ‘flow’ sample or retaining on the beads (bound to streptavidin beads, but not eluted) are as expected. For example, the RNase A (-) treated sample had 99% of RNA recovery in the ‘flow’ sample indicating

that there were minimal to no RNA that was biotinylated. On the other hand, the MTS-xx csRNA sample had only 87% of the RNA found in 'flow' sample while the other 13% stayed within the column. Furthermore, the positive controls of 4sU+MTS-biotin RNA and ssDNA-biotin showed a much larger percentage of RNA stuck on the beads, being 58% and 87% respectively. The percentages indicating the nucleotides "stuck" on the streptavidin-coated magnetic beads should be those biotinylated molecules. The amount of RNA

Figure 16:

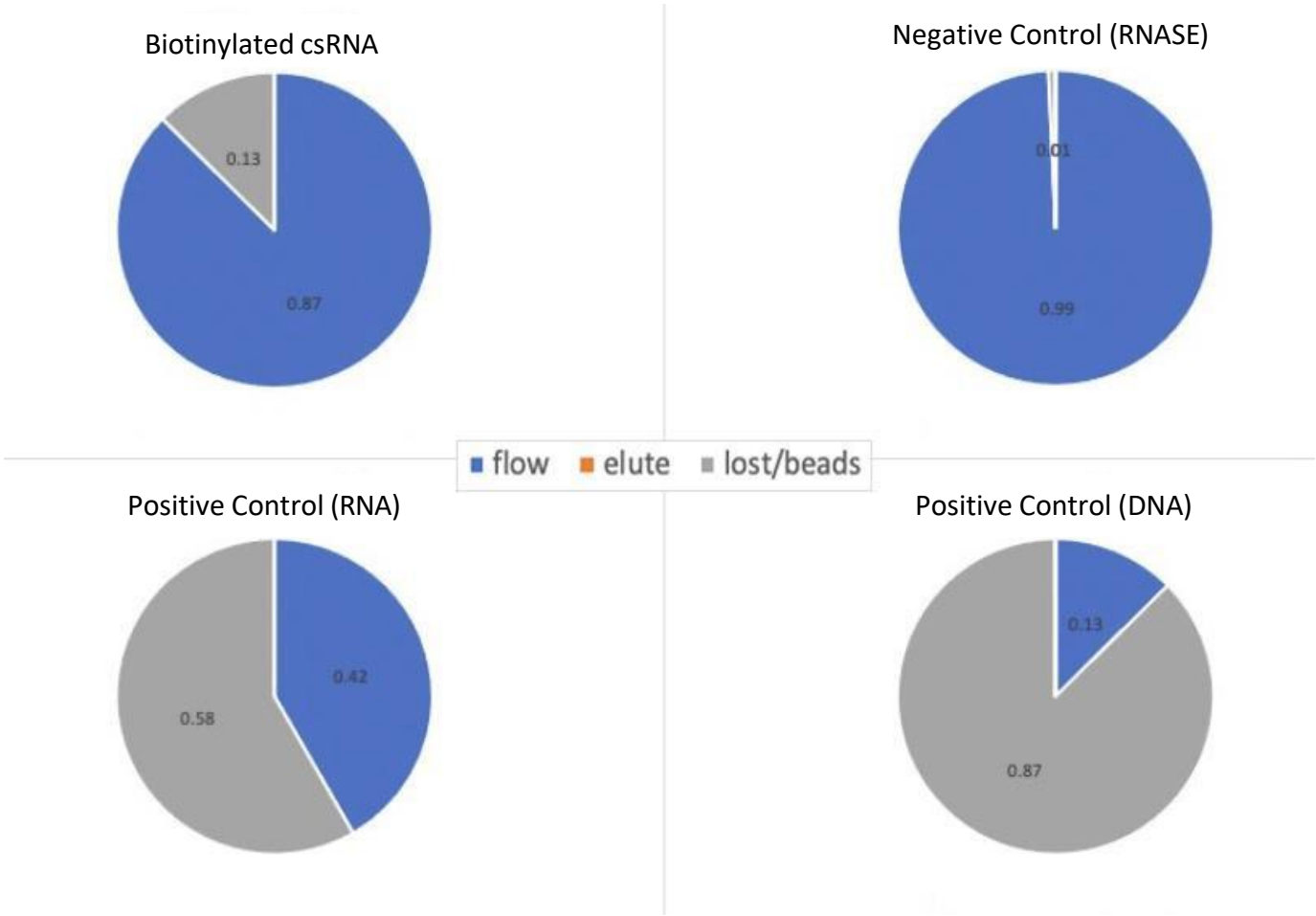

Fig. 16: Initial uMACS separation trial with experimental csRNA sample, negative control (RNASE) treated sample, positive controls (RNA and DNA). The trend of biotinylated RNA percentages retaining bound to the magnetic beads directly represents the efficiency of biotinylating in each sample

biotinylated within each sample are ranked as expected. RNase (- control) sample had the least amount of biotinylated RNA, csRNA sample had a small percentage of biotinylated RNA, and the positive control had the most biotinylated RNA.

In order to troubleshoot the elution process, a variety of different elution buffers with altered concentrations, pH's, and reducing agents were used. In addition to the 100mM DTT elution initially used, 100mM Tris (2-carboxyethyl) phosphine (TCEP), 100 ug/ml RNase A, 100 ug/ml Proteinase K, and 25mM biotin were also tested to see if any RNA could be eluted from the positive control samples. The rationale behind using Proteinase K is to degrade the streptavidin coated on the magnetic beads to elute the full biotinylated RNA sample. Further reduction and protein purification steps could be then performed on the eluted RNA sampling before subjecting it to RNA sequencing. RNase A elution was used for confirmation that the expected biotinylated RNA is in fact stuck to the columns and could not be used for further applications. High concentrations of biotin could also elute the biotinylated samples by replacing the RNA biotin-streptavidin interaction. Like using proteinase K, using biotin would require further reducing and RNA purification steps before sequencing. Unfortunately, the results were very similar to the initial findings represented in Figure 15. None of these gave optimal elution (data not shown). The highest percentage of elution sample calculated resulted from the RNase elution at ~4% eluted RNA from a positive control (measured via Qbit). Although this is a signal that the RNase A elution buffer could force some of the RNA out of the column, much of the RNA stayed bound to the streptavidin coated magnetic beads.

Due to the difficulty of troubleshooting this process, a hypothesis was developed trying to explain why the majority of RNA was staying bound to the magnetic beads. All samples that

were used to create positive controls underwent 4sU incubation overnight. An overnight incubation of 4sU could mean that more 4sU would be incorporated per RNA transcript. If this is true, then each RNA transcript could obtain multiple MTSEA crosslinkers. This means that each RNA transcript would acquire an abundance of biotin crosslinkers. Then, when applying the highly biotinylated RNA to the streptavidin coated uMACS beads, multi-covalent binding could occur, therefore wrapping the RNA transcripts tighter to the beads as depicted in Figure 17.

Figure 17:

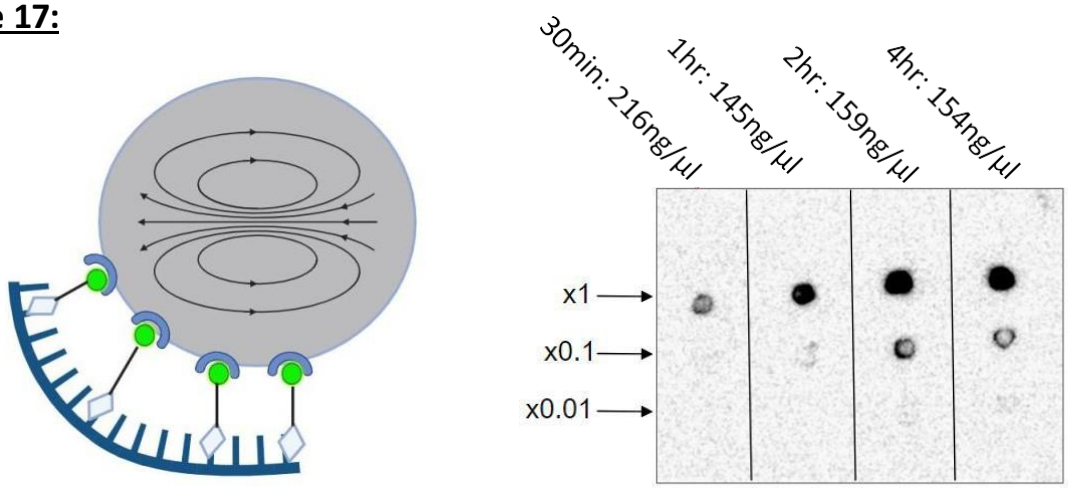

Fig. 17: Left – schematic representing new hypothesis of multivalent binding of over biotinylated RNA samples. Right – Dot Blot showing detection signal intensities are directly related to 4sU incubation times in-vitro.

With this possibility in mind, the incubation time for 4sU incorporation was lowered to a range of 30 minutes to 4 hours. This resulted in a dot blot shown in Figure 16, clearly indicating that decreased incubation time of 4sU leads to a weaker biotin detection in the Dot Blot.

These positive control samples were then directly used for troubleshooting the uMACS separation procedure. As shown in Figure 17, although the 4hr-4sU-incubation sample showed

less total RNA binding to the streptavidin beads, there were no eluted RNA from the samples using 100mM DTT. These results were uniform across all the different 4sU incubation times (30min, 1hr, 1hr). Practically, 4sU incubation any less than overnight might not be long enough to label csRNA, because the dynamics and mechanism involved in transporting newly transcribed RNA to the cell surface is unknown.

Figure 16:

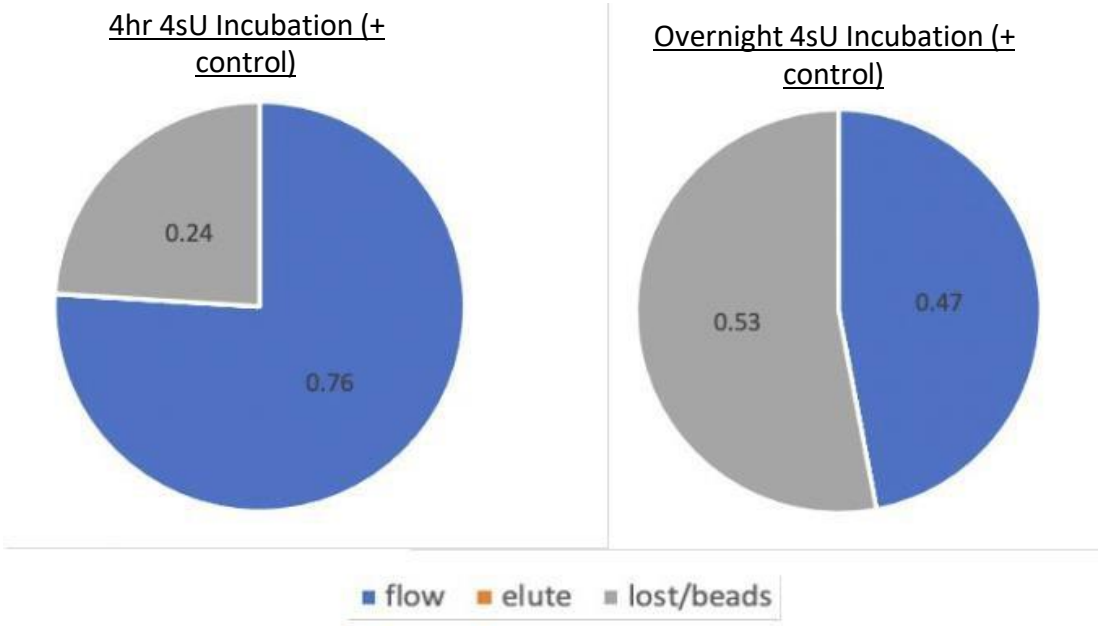

Fig. 17: 4hr 4sU incubation time made into positive controls and then attempted to separate in uMACS procedure. Amount of RNA residing on the beads was less due to less biotinylating, however, no elution RNA sample detected.

2.2 Using Ultra-Performance Liquid Chromatography to Verify Crosslinking Chemistry Between 4sU Monomer and MTSEA Crosslinkers and its Reversibility by DTT Reduction Used in Elution

This prominent roadblock for the separation procedure steered us to confirm the chemistry behind 4sU+ and MTSEA-biotin crosslinking. Additionally, there was a need to make sure reducing agents like DTT could reduce the di-sulfide bond created from the crosslinking reaction. To do this, Ultra Performance Liquid Chromatography (UPLC) method was applied. First, standards of each molecule were run through the reverse phase column (1mg/ml MTSEA-xx-biotin and 1mg/ml 4sU monomer). The mass to charge ratio graphs in Figure 18 represent these standards. If there is peak showing distinct intensity at a certain mass, then there is confidence that a molecule of that size was detected. The addition of a proton during mass spectrometry will add an additional unit to the mass of each compound. For example, in Figure 18, we see a distinct peak at the 608 mass to charge ratio. Since MTSEA-xx-biotin has a molecular weight of 607, we can confidently identify this peak as MTSEA-xx-biotin detection. Again, since the molecular weight of 4sU is 260, the peak found at the mass to charge ratio of 261 represents 4sU. There also was an observable peak at a charge to mass ratio of 283. It is speculated that this is also 4sU but charged with a sodium ion (mw of 23) instead of a proton.

Figure 18:

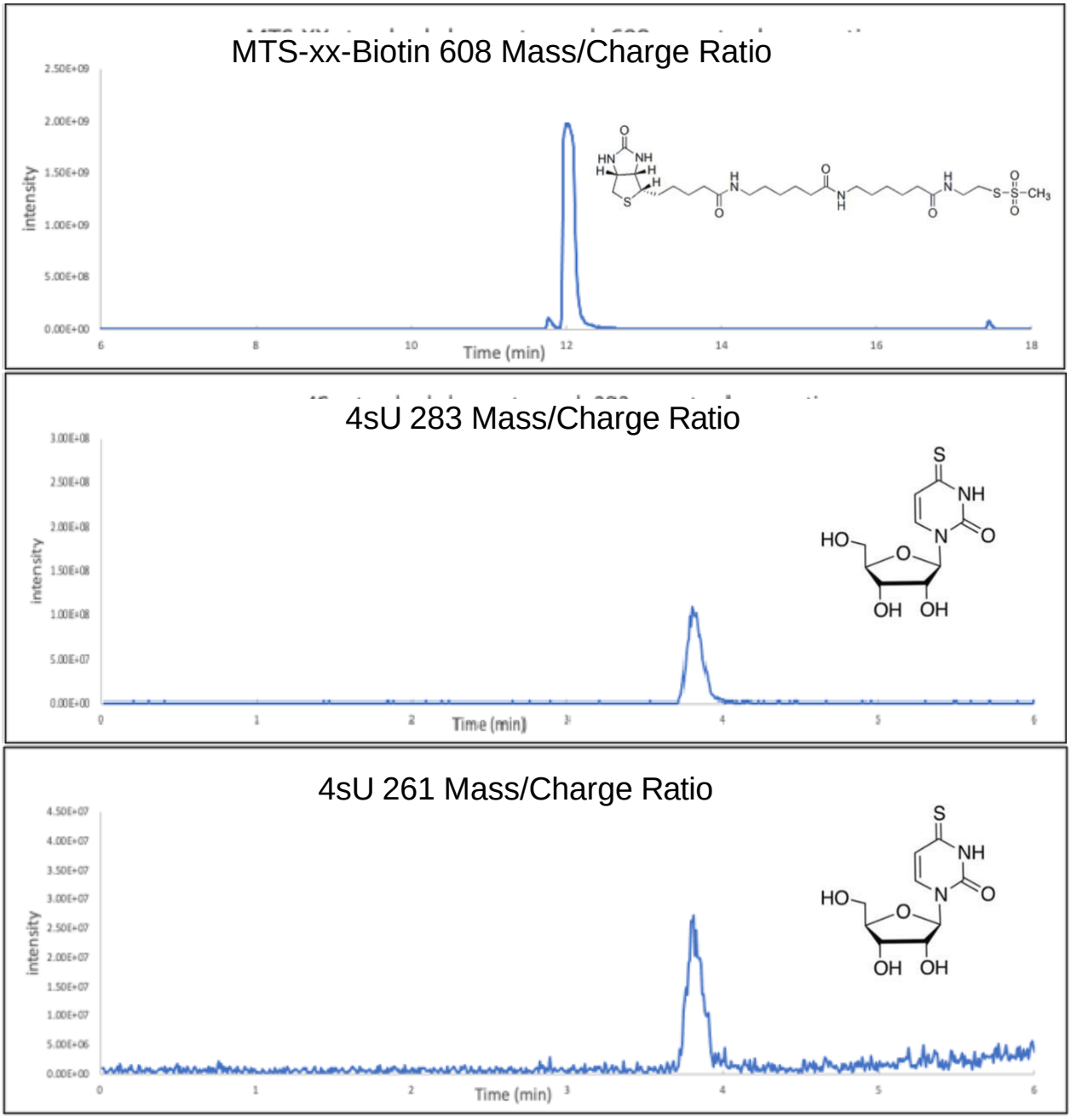

Fig. 18: 4sU standard and MTSEA-xx-biotin standard ran through UPLC and detected via Mass Spec to identify mass to charge ratio peaks.

After the standards were measured, a sample of the crosslinking reaction was applied to the same UPLC procedure. These results are shown in Figure 19.1 and 19.2. The mass to charge ratio representing 4sU (261 and 283) were completely diminished. There was some extra MTSEA-xx-biotin compound observed in the sample at a mass to charge ratio of 608. The clear peak intensity representing a cross-linked product at mass to charge ratio of 788 was also observed. The mass to charge ratio of the crosslinked is 788 and not 868 due to the loss of methanesulfonyl (mw of 80).

Figure 19.1:

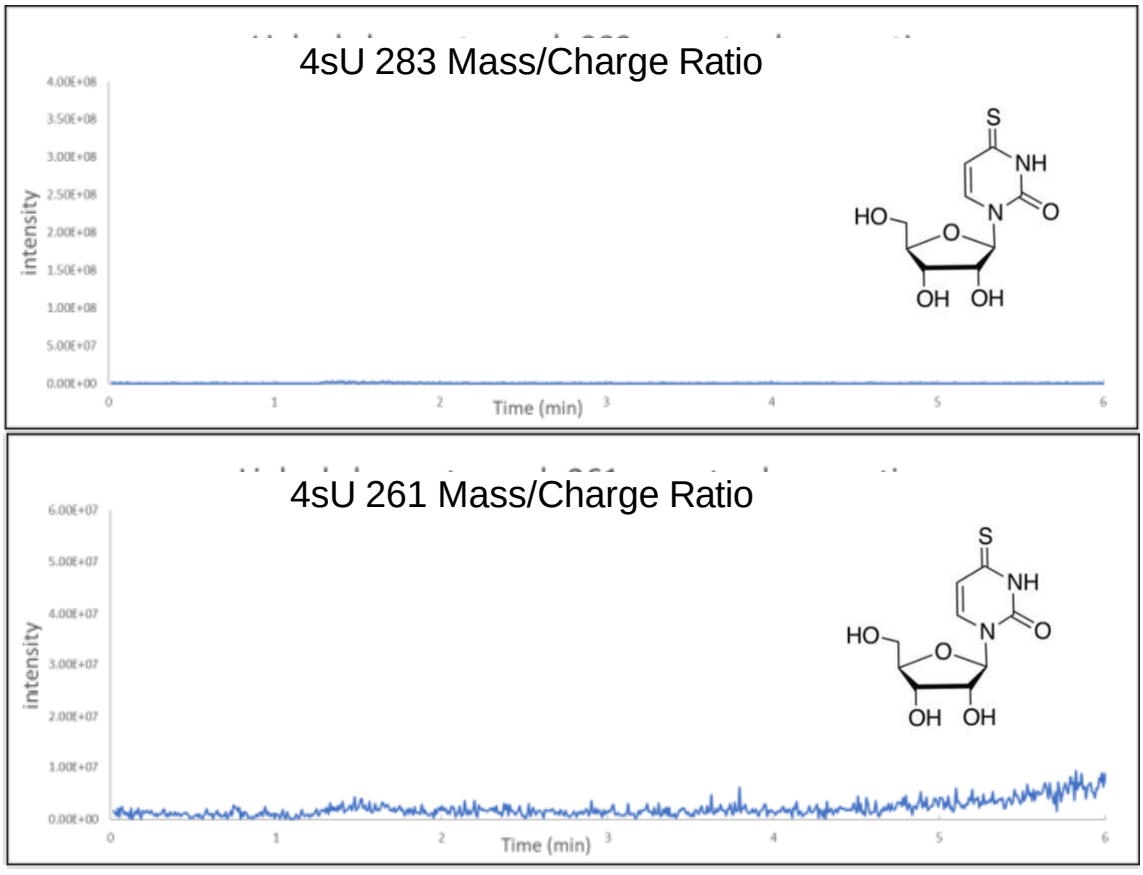

(Rest of figure and description on next page)

Figure 19.2:

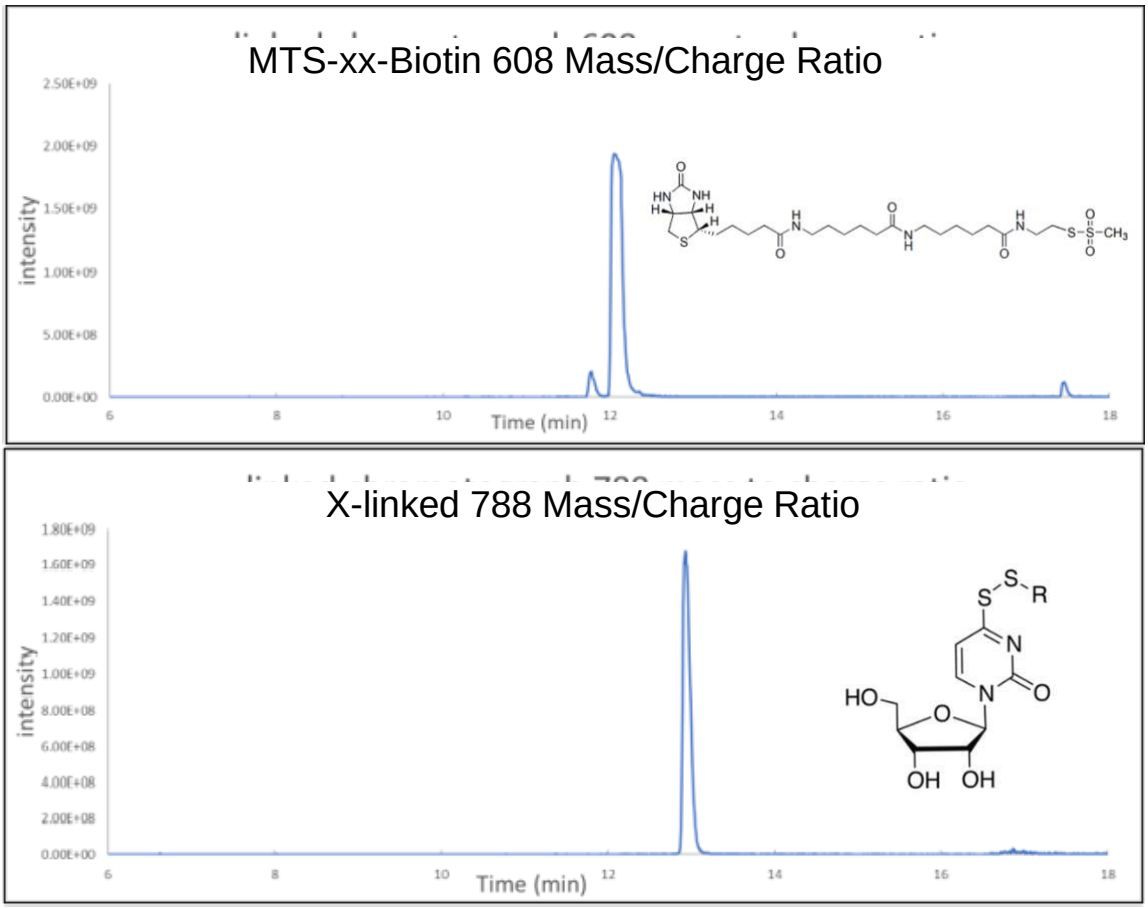

Fig. 19: Resulting compounds identified from crosslinking reaction. 4sU charge to mass ratios of 283 and 261 were completely lost, and residual MTSEA-xx-biotin compound was identified via 608 mass to charge ratio peak. A new peak found at 788 indicates 4sU+MTSEA-xx-biotin crosslinking molecule.

Lastly, an addition of 100mM DTT was added to the mixture of both the 4sU monomer and MTSEA-xx-biotin crosslinker. This was done to see if DTT could disrupt the 788 mass to charge ratio signal, indicating that the two compounds were reduced and separated from one another. The results are represented in Figure 20. There was a slight return of the peaks representing the 4sU monomer at a mass to charge ratio of 261 and 283. The 608 mass to charge ratio peak of MTSEA-xx-biotin stayed consistent. Most importantly, the 788 mass to charge ratio

peak was completely diminished, representing that the DTT has separated the crosslinked compound.

Figure 20:

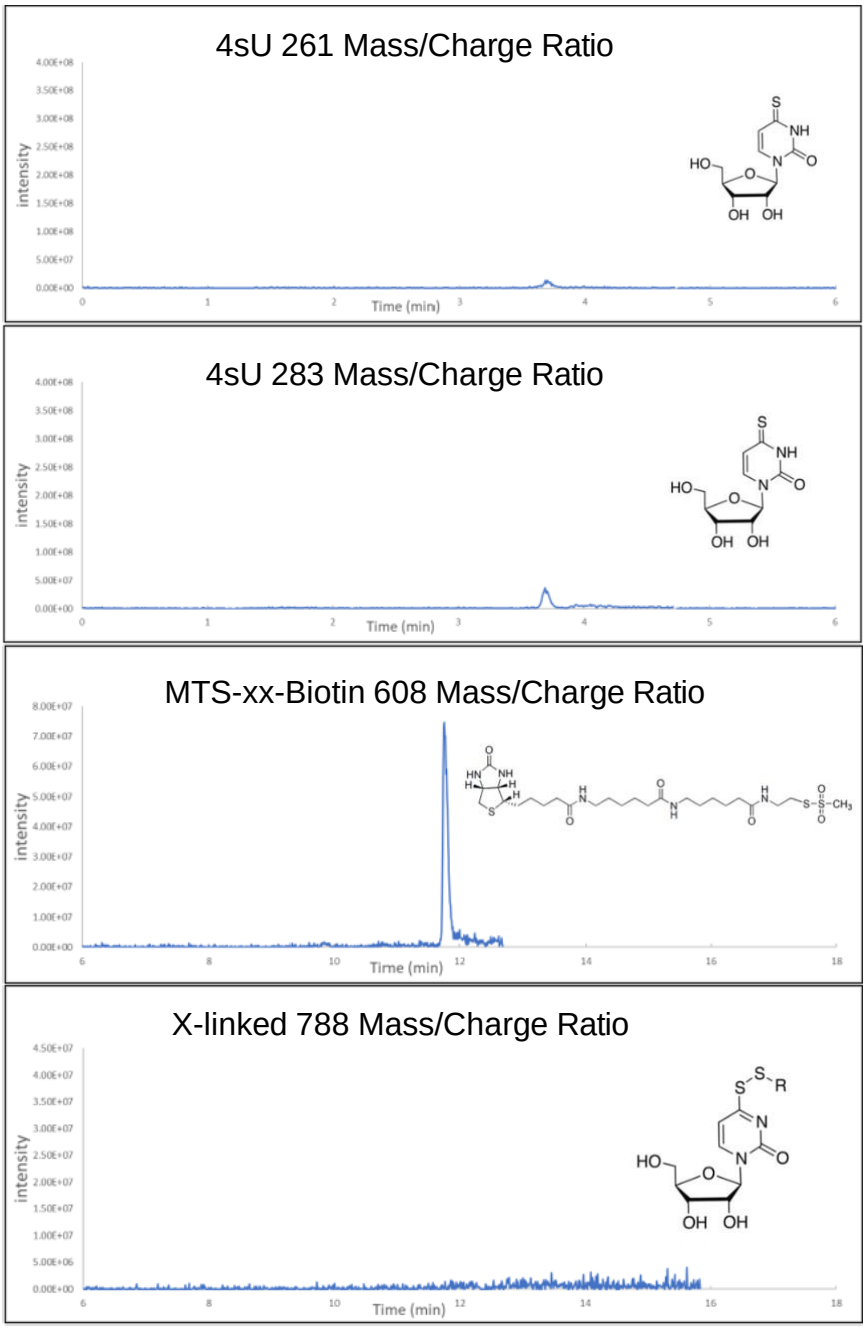

Fig. 20: Crosslinking reaction sample spiked with DTT reducing agent to test reversibility of click chemistry. 261 and 283 mass to charge ratio peaks reappeared indicating 4sU monomer cleavage from MTSEA-xx-biotin crosslinker. Depletion of 788 mass to charge ratio peak shows crosslinked molecule no longer exists after DTT reduction.

Therefore, the crosslinking chemistry, and the reversibility of this covalent reaction using a reducing agent such as DTT have been confirmed. Elution problems observed in uMACS separation are not due to the reagents being used, but unknown biochemical properties between 4sU+ RNA and MTSEA-xx-biotin could be causing the problems associated with separation.

Discussion/Future Directions:

The dot blots represented in Figure 14 and Figure 15 indicated that MTSEA-xx-biotin is crosslinking with csRNA. HeLa cells have been the only csRNA that has been detected. Successfully expanding this procedure to HEK293T cells and EL4 suspension cells can further support this claim. However, there are still concerns with the results involving HeLa cells. Sensitivity and reproducibility continue to be an issue with detecting csRNA. Having the total RNA concentration to be above 3ug/μμ is desirable to detect csRNA. Additionally, larger blot sizes (>5ul rather than 2ul) has shown to strengthen detection signal. Using 800 grit sandpaper has sped up the absorption time it takes for samples to dry on the nylon membrane and should continue to be practiced for it has reduced background noise as well. Making sure the membranes are washed for the full 10 minutes 2x for each buffer is important to ensure minimal background noise along the edges of the membrane. For detecting csRNA and comparing it to the RNase (-) counterpart, RNase A incubation on the mammalian cell cultures needs to be optimized. Interestingly in (Ma et al., 2023), they describe how glycoRNAs are much more resistant to degradation via RNase A compared to non-modified csRNA. This could explain the resulting blot seen in Figure 15, where the MTS-xx-biotin crosslinker is labeling all csRNA in the experimental sample and only glycoRNA in the RNase A (-) sample due to their resistance to the

enzyme. Using different RNase A products (from powder, not already resuspended solution) may fix the enzymes efficiency. Additionally, ensuring high viability of the mammalian cells before adding the MTSEA-xx-biotin crosslinker is essential to keep the crosslinker from interacting with intercellular RNA. It is mentioned in (Flynn et al., 2021) that α2-3,6,8,9-neuraminidase A can cleave the glycan moiety of glycoRNAs, which could be used to test this theory in relation to the Figure 15 results. Diligence and patience with the washing steps is also crucial to rid cell culture from any free MTSEA-xx-biotin before lysing the cells for RNA isolation.

RNA separation procedure has been the largest roadblock to progress. The nature of biotinylated RNA binding to the streptavidin coated beads, but not being eluted by the variety of different buffers tried, has been very persistent. However, uMACS is not the only magnetic separation process of biotinylated molecules. Other companies also provide similar methods utilizing the same principle. DynaBeads have also been used to try and separate biotinylated RNA from non-biotinylated RNA, but the results have been almost identical when using DTT as the reducing agent. It may be worthwhile to try the different elutions (such as Biotin, RNase A, and proteinase K) on the DynaBeads as well. Additionally, a different range of pHs have been used for both uMACS and DynaBead optimization but increasing the temperature of the elution reaction has only been performed on uMACS beads. DynaBead elution incubations have yet to be subjected to increased temperatures. UPLC data has confirmed that the crosslinked reactions of the 4sU monomer and MTSEA-xx-biotin crosslinker can be reduced via DTT. However, 4sU do not represent full RNA transcripts with incorporated 4sU. The addition of RNA into the reaction could have biochemical properties that are disrupting the reaction's reversibility in order to elute biotinylated RNA from streptavidin coated magnetic beads. Furthermore, the streptavidin

coated beads could be restricting the reducing agents as well. It may be likely that the addition of RNA and magnetic beads could cause steric hindrance of the DTT reducing agent, therefore DTT cannot reach the disulfide bond. Instead of using MTSEA crosslinkers to create a positive control, HPDP could be used (previously established crosslinker for labeling RNA with similar reversibility using DTT) (Duffy et al., 2015). This would confirm that the elution problem is due to the MTSEA crosslinkers and not the procedure itself.

The addition of using MTSEA-fluorophore crosslinkers for visualizing the csRNA on mammalian cell cultures would be a great confirmation that csRNA can be detected via MTSEA click chemistry. Biotium has a few different MTSEA-fluorophores available commercially (Biotium Cat no. 92097). Similarly to crosslinking csRNA with MTSEA-biotin, MTSEA-fluorophores can be applied after mammalian cells are treated with proteinase K (Flynn et al., 2021; Ma et al., 2023; Zhang et al., 2024). Due to MTSEA crosslinking occurring at any free sulfhydryl groups, MTSEA-fluorphore crosslinkers could react with cysteines presented on cell membrane proteins creating a false positive . Therefore, proteinase K is a crucial step during this process. Adding this procedure could verify MTSEA crosslinkers are specific for labeling csRNA on mammalian cell cultures (HeLa, HEK293T, EL4), and provide imaging for visualization of this labeling technique.

Studying cell surface RNA will eventually require isolating it from the more abundant internal RNA within a cell population. Once isolated, these RNAs will need to be sequenced using traditional methods like next-generation sequencing to identify their origin and potential functions(J. Wang et al., 2024; Z. Wang et al., 2009) . Since cell surface RNAs often undergo chemical modifications, mass spectrometry (MS) can be a complementary technique. MS alongside RNA sequencing will help reveal the specific modifications, functions, and structures of

these external RNA molecules providing insights into their stability and regulatory roles (Lauman & Garcia, 2020; Wetzel & Limbach, 2016).

The significance of this research feeds into two different future applications. Basic biological research of csRNA has only recently began (Flynn et al., 2021; Lv et al., 2023; Ma et al., 2023; Zhang et al., 2024), and novel methods for streamlining the process of characterizing csRNA, uncovering their structure, and describing their function will greatly improve the field. It is clear that csRNA has an important biological role in certain tissues and may even play a crucial role in the immune response (Lv et al., 2023; Zhang et al., 2024). Further establishing these methods will provide the means to quickly explore these roles that csRNA have in cell adhesion/localization, immune activation, and cell-cell communication.

csRNA also presents a unique opportunity for directed therapeutic delivery. As different tissues containing csRNA get sequenced and profiled, there seems to be a uniqueness and uniformity to csRNA sequences on these cell types (Chai et al., 2023; Flynn et al., 2021; Huang et al., 2020; Lv et al., 2023). In other words, depending on the type of tissue, specific csRNA sequences may be overexpressed on one cell type and not found on other cell types. These sequences, or “molecular zip-codes”, presented on the cell surface could be used to deliver drugs targeting one cell type while avoiding other non-targets. This is especially of interest when discussing possible therapeutics for cancer or autoimmune therapy (Jong & Kocer, 2023; Roslan et al., 2022). Delivering cytotoxic drugs to only cancer tissue and/or immune cells with overexpressed csRNA may be the key to future cancer therapies and/or controlling autoimmune diseases respectively (Pisetsky, 2023; Saito et al., 2017).

References

Aranda, P. S., Lajoie, D. M., & Jorcyk, C. L. (2012). Bleach gel: A simple agarose gel for analyzing RNA quality. *Electrophoresis*, *33*(2), 366–369. https://doi.org/10.1002/elps.201100335

Block, K. F., Puerta-Fernandez, E., Wallace, J. G., & Breaker, R. R. (2011). Association of OLE RNA with bacterial membranes via an RNA-protein interaction. *Molecular Microbiology*, *79*(1), 21–34. https://doi.org/10.1111/j.1365-2958.2010.07439.x

Casciola-Rosen, L. A., Anhah, G., & Rosen~, A. (n.d.). *Autoantigens Targeted in Systemic Lupus Erythematmus Are Clustered in Two Populations of Surface Structures on Apoptotic Keratinocytes*. http://rupress.org/jem/article-pdf/179/4/1317/1675782/1317.pdf

Chai, P., Lebedenko, C. G., & Flynn, R. A. (2023). *Annual Review of Genomics and Human Genetics RNA Crossing Membranes: Systems and Mechanisms Contextualizing Extracellular RNA and Cell Surface GlycoRNAs*. https://doi.org/10.1146/annurev-genom-101722

Chomczynski, P., & Sacchi, N. (2006a). The single-step method of RNA isolation by acid guanidinium thiocyanate-phenol-chloroform extraction: Twenty-something years on. *Nature Protocols*, *1*(2), 581–585. https://doi.org/10.1038/nprot.2006.83

Chomczynski, P., & Sacchi, N. (2006b). The single-step method of RNA isolation by acid guanidinium thiocyanate-phenol-chloroform extraction: Twenty-something years on. *Nature Protocols*, *1*(2), 581–585. https://doi.org/10.1038/nprot.2006.83

Duffy, E. E., Rutenberg-Schoenberg, M., Stark, C. D., Kitchen, R. R., Gerstein, M. B., & Simon, M. D. (2015). Tracking Distinct RNA Populations Using Efficient and Reversible Covalent Chemistry. *Molecular Cell*, *59*(5), 858–866. https://doi.org/10.1016/j.molcel.2015.07.023

Flynn, R. A., Pedram, K., Malaker, S. A., Batista, P. J., Smith, B. A. H., Johnson, A. G., George, B. M., Majzoub, K., Villalta, P. W., Carette, J. E., & Bertozzi, C. R. (2021). Small RNAs are modified with N-glycans and displayed on the surface of living cells. *Cell*, *184*(12), 3109-3124.e22. https://doi.org/10.1016/j.cell.2021.04.023

Garibaldi, A., Carranza, F., & Hertel, K. J. (2017). Isolation of newly transcribed rna using the metabolic label 4-thiouridine. In *Methods in Molecular Biology* (Vol. 1648, pp. 169–176). Humana Press Inc. https://doi.org/10.1007/978-1-4939-7204-3_13

Harris, M. E., & Christian, E. L. (2009). RNA crosslinking methods. *Methods in Enzymology*, *468*, 127–146. https://doi.org/10.1016/s0076-6879(09)68007-1

Huang, N., Fan, X., Zaleta-Rivera, K., Nguyen, T. C., Zhou, J., Luo, Y., Gao, J., Fang, R. H., Yan, Z., Chen, Z. B., Zhang, L., & Zhong, S. (2020). Natural display of nuclear-encoded RNA on the cell surface and its impact on cell interaction. *Genome Biology*, *21*(1). https://doi.org/10.1186/s13059-020-02145-6

Jong, E. de, & Kocer, A. (2023). Current Methods for Identifying Plasma Membrane Proteins as Cancer Biomarkers. In *Membranes* (Vol. 13, Issue 4). MDPI. https://doi.org/10.3390/membranes13040409

Lamandé Editor, S. R. (2018). *mRNA Decay Methods and Protocols Methods in Molecular Biology 1720*. http://www.springer.com/series/7651

Lauman, R., & Garcia, B. A. (2020). Unraveling the RNA modification code with mass spectrometry. In *Molecular Omics* (Vol. 16, Issue 4, pp. 305–315). Royal Society of Chemistry. https://doi.org/10.1039/c8mo00247a

Lewis, M. R., Pearce, J. T. M., Spagou, K., Green, M., Dona, A. C., Yuen, A. H. Y., David, M., Berry, D. J., Chappell, K., Horneffer-Van Der Sluis, V., Shaw, R., Lovestone, S., Elliott, P., Shockcor, J., Lindon, J. C., Cloarec, O., Takats, Z., Holmes, E., & Nicholson, J. K. (2016). Development and Application of Ultra-Performance Liquid Chromatography-TOF MS for Precision Large Scale Urinary Metabolic Phenotyping. *Analytical Chemistry*, *88*(18), 9004–9013. https://doi.org/10.1021/acs.analchem.6b01481

Li, X., Ben-Dov, I. Z., Mauro, M., & Williams, Z. (2015a). Lowering the quantification limit of the QubitTM RNA HS Assay using RNA spike-in. *BMC Molecular Biology*, *16*(1). https://doi.org/10.1186/s12867-015-0039-3

Li, X., Ben-Dov, I. Z., Mauro, M., & Williams, Z. (2015b). Lowering the quantification limit of the QubitTM RNA HS Assay using RNA spike-in. *BMC Molecular Biology*, *16*(1). https://doi.org/10.1186/s12867-015-0039-3

Lv, J., Liu, Y., Tang, J., Xiao, H., Hu, R., Wang, G., Niu, D., Shao, P. L., Yang, J., Jin, Z., Xu, Z., & Zhang, B. (2023). A Novel Cell Membrane-Associated RNA Extraction Method and Its Application in the Discovery of Breast Cancer Markers. *Analytical Chemistry*, *95*(31), 11706–11713. https://doi.org/10.1021/acs.analchem.3c01689

Ma, Y., Guo, W., Mou, Q., Shao, X., Lyu, M., Garcia, V., Kong, L., Lewis, W., Ward, C., Yang, Z., Pan, X., Yi, S. S., & Lu, Y. (2023). Spatial imaging of glycoRNA in single cells with ARPLA. *Nature Biotechnology*. https://doi.org/10.1038/s41587-023-01801-z

Manya, H., Yamaguchi, Y., Kanagawa, M., Kobayashi, K., Tajiri, M., Akasaka-Manya, K., Kawakami, H., Mizuno, M., Wada, Y., Toda, T., & Endo, T. (2016). The muscular dystrophy gene TMEM5 encodes a ribitol ô1,4-Xylosyltransferase required for the functional

glycosylation of dystroglycan. *Journal of Biological Chemistry*, *291*(47), 24618–24627. https://doi.org/10.1074/jbc.M116.751917

Mattick, J. S., Amaral, P. P., Carninci, P., Carpenter, S., Chang, H. Y., Chen, L. L., Chen, R., Dean, C., Dinger, M. E., Fitzgerald, K. A., Gingeras, T. R., Guttman, M., Hirose, T., Huarte, M., Johnson, R., Kanduri, C., Kapranov, P., Lawrence, J. B., Lee, J. T., … Wu, M. (2023). Long non-coding RNAs: definitions, functions, challenges and recommendations. *Nature Reviews Molecular Cell Biology*, *24*(6), 430–447. https://doi.org/10.1038/s41580-022-00566-8

Morozkin, E. S., Laktionov, P. P., Rykova, E. Y., & Vlassov, V. V. (2004). Extracellular nucleic acids in cultures of long-term cultivated eukaryotic cells. *Annals of the New York Academy of Sciences*, *1022*, 244–249. https://doi.org/10.1196/annals.1318.038

nylm-ro. (n.d.).

Pisetsky, D. S. (2023). Pathogenesis of autoimmune disease. In *Nature Reviews Nephrology* (Vol. 19, Issue 8, pp. 509–524). Nature Research. https://doi.org/10.1038/s41581-023-00720-1

Praissman, J. L., Willer, T., Osman Sheikh, M., Toi, A., Chitayat, D., Lin, Y. Y., Lee, H., Stalnaker, S. H., Wang, S., Prabhakar, P. K., Nelson, S. F., Stemple, D. L., Moore, S. A., Moremen, K. W., Campbell, K. P., & Wells, L. (2016). The functional O-mannose glycan on α-dystroglycan contains a phospho-ribitol primed for matriglycan addition. *ELife*, *5*(APRIL2016). https://doi.org/10.7554/eLife.14473

Rabani, M., Levin, J. Z., Fan, L., Adiconis, X., Raychowdhury, R., Garber, M., Gnirke, A., Nusbaum, C., Hacohen, N., Friedman, N., Amit, I., & Regev, A. (2011). Metabolic labeling of RNA

uncovers principles of RNA production and degradation dynamics in mammalian cells. *Nature Biotechnology*, *29*(5), 436–442. https://doi.org/10.1038/nbt.1861

Ren, L., Liu, L., Hu, S., Zhu, Z., Zhu, H., Ma, J., Zhao, X., Wang, X., Zhang, C., Gu, M., & Li, X. (2018). Improved dot blotting for small RNA detection. *Acta Biochimica et Biophysica Sinica*, *50*(12), 1294–1296. https://doi.org/10.1093/abbs/gmy135

Roslan, A., Sulaiman, N., Mohd Ghani, K. A., & Nurdin, A. (2022). Cancer-Associated Membrane Protein as Targeted Therapy for Bladder Cancer. In *Pharmaceutics* (Vol. 14, Issue 10). MDPI. https://doi.org/10.3390/pharmaceutics14102218

Saito, R., Abe, H., Kunita, A., Yamashita, H., Seto, Y., & Fukayama, M. (2017). Overexpression and gene amplification of PD-L1 in cancer cells and PD-L1 + immune cells in Epstein-Barr virus-associated gastric cancer: The prognostic implications. *Modern Pathology*, *30*(3), 427–439. https://doi.org/10.1038/modpathol.2016.202

Söderberg, O., Gullberg, M., Jarvius, M., Ridderstråle, K., Leuchowius, K. J., Jarvius, J., Wester, K., Hydbring, P., Bahram, F., Larsson, L. G., & Landegren, U. (2006). Direct observation of individual endogenous protein complexes in situ by proximity ligation. *Nature Methods*, *3*(12), 995–1000. https://doi.org/10.1038/nmeth947

Tavoosidana, G., Ronquist, G., Darmanis, S., Yan, J., Carlsson, L., Wu, D., Conze, T., Ek, P., Semjonow, A., Eltze, E., Larsson, A., Landegren, U. D., & Kamali-Moghaddam, M. (2011). Multiple recognition assay reveals prostasomes as promising plasma biomarkers for prostate cancer. *Proceedings of the National Academy of Sciences of the United States of America*, *108*(21), 8809–8814. https://doi.org/10.1073/pnas.1019330108

Tsuji, Y. (2023). Optimization of Biotinylated RNA or DNA Pull-Down Assays for Detection of Binding Proteins: Examples of IRP1, IRP2, HuR, AUF1, and Nrf2. *International Journal of Molecular Sciences*, *24*(4). https://doi.org/10.3390/ijms24043604

Vennapusa, A. R., Somayanda, I. M., Doherty, C. J., & Jagadish, S. V. K. (2020). A universal method for high-quality RNA extraction from plant tissues rich in starch, proteins and fiber. *Scientific Reports*, *10*(1). https://doi.org/10.1038/s41598-020-73958-5

Wang, D., & Farhana, A. (2023). *Biochemistry, RNA Structure* . StatPearls.

Wang, J., Zhang, Y., Zhang, T., Tan, W. T., Lambert, F., Darmawan, J., Huber, R., & Wan, Y. (2024). RNA structure profiling at single-cell resolution reveals new determinants of cell identity. *Nature Methods*, *21*(3), 411–422. https://doi.org/10.1038/s41592-023-02128-y

Wang, Z., Gerstein, M., & Snyder, M. (2009). RNA-Seq: A revolutionary tool for transcriptomics. In *Nature Reviews Genetics* (Vol. 10, Issue 1, pp. 57–63). https://doi.org/10.1038/nrg2484

Wetzel, C., & Limbach, P. A. (2016). Mass spectrometry of modified RNAs: Recent developments. In *Analyst* (Vol. 141, Issue 1, pp. 16–23). Royal Society of Chemistry. https://doi.org/10.1039/c5an01797a

Xie, Y., Dang, W., Zhang, S., Yue, W., Yang, L., Zhai, X., Yan, Q., & Lu, J. (2019). The role of exosomal noncoding RNAs in cancer. In *Molecular Cancer* (Vol. 18, Issue 1). BioMed Central Ltd. https://doi.org/10.1186/s12943-019-0984-4

Xu, T.-H., Yan, Y., G. Harikumar, K., & J. Miller, L. (2017). Streptavidin bead pulldown assay to determine homooligomerization. *BIO-PROTOCOL*, *7*(24). https://doi.org/10.21769/bioprotoc.2901

Yue, H., Chen, J., Chen, X., Wang, X., Zhang, Y., & Zhou, N. (2021). Systematic screening and optimization of single-stranded DNA aptamer specific for N-acetylneuraminic acid: A comparative study. *Sensors and Actuators, B: Chemical*, *344*. https://doi.org/10.1016/j.snb.2021.130270

Zhang, N., Tang, W., Torres, L., Wang, X., Ajaj, Y., Zhu, L., Luan, Y., Zhou, H., Wang, Y., Zhang, D., Kurbatov, V., Khan, S. A., Kumar, P., Hidalgo, A., Wu, D., & Lu, J. (2024). Cell surface RNAs control neutrophil recruitment. *Cell*, *187*(4), 846-860.e17. https://doi.org/10.1016/j.cell.2023.12.033